ACS Pharmacology & Translational Science

pubs.acs.org/ptsci
Article

Identification of a Compound Inhibiting Both the Enzymatic and Nonenzymatic Functions of Indoleamine 2,3-Dioxygenase 1

Eleonora Panfili, Sarah Jane Rezzi, Annalisa Adamo, Daniele Mazzoletti, Alberto Massarotti, Riccardo Miggiano, Silvia Fallarini, Sara Ambrosino, Alice Coletti, Pasquale Molinaro, Michele Milella, Salvatore Paiella, Antonio Macchiarulo, Stefano Ugel, Tracey Pirali,* and Maria Teresa Pallotta*

Cite This: ACS Pharmacol. Transl. Sci. 2024, 7, 3056−3070

Read Online

ACCESS | Metrics & More | Article Recommendations | Supporting Information

ABSTRACT: Indoleamine 2,3-dioxygenase 1 (IDO1) plays a key role in tumor immune escape. Besides being a metabolic enzyme that catalyzes the first step of tryptophan catabolism, it also acts as a signal-transducing protein, whose partnering with tyrosine phosphatase Src homology 2 (SH2) domain-containing protein tyrosine phosphatase substrate (SHPs) and phosphatidylinositol-3-kinase (PI3K) regulatory subunit p85 promotes the establishment of a sustained immunosuppressive phenotype. While IDO1 inhibitors typically interfere with its enzymatic activity, we aimed to discover a more effective modulator capable of blocking not only the enzymatic but also the signaling-mediated functions of IDO1. By virtual screening, we identified the compound VS-15, which selectively binds the heme-free form of IDO1, inhibits its enzymatic activity, and reduces the IDO1-mediated signaling pathway by negatively interfering with its partnership with SHPs and PI3K regulatory subunit p85 as well as with the IDO1 anchoring to the early endosomes in tumor cells. Moreover, VS-15 counteracts the TGF-β—mediated immunosuppressive phenotype in dendritic cells and reduces the level of inhibition of T cell proliferation by suppressive monocytes isolated from patients affected by pancreatic cancer. Herein, we describe the discovery and characterization of a small molecule with an unprecedented mechanism of action, capable of inhibiting both the enzymatic and nonenzymatic activities of IDO1 by binding to its apo-form. These results pave the way for the development of next-generation IDO1 inhibitors with a unique competitive advantage over the currently available modulators, thereby opening therapeutic opportunities in cancer immunotherapy.

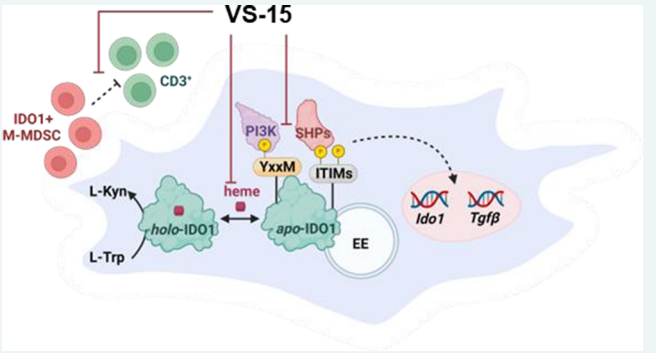

KEYWORDS: *indoleamine 2,3-dioxygenase 1 (IDO1), heme, kynurenine, nonenzymatic activity, IDO1 inhibitor, cancer immunotherapy*

Indoleamine 2,3-dioxygenase 1 (IDO1) is an immune checkpoint protein that orchestrates immune responses in multiple physio-pathological contexts. IDO1 is mostly expressed in dendritic cells (DCs), antigen-presenting cells (APCs) in which IDO1 induces immunosuppressive responses by relying on both enzymatic and nonenzymatic activity.[1] As illustrated in Figure 1A, in its heme-containing form (holo-IDO1), IDO1 catalyzes the oxidative cleavage of the indole ring in L-tryptophan (Trp). By regulating the catabolism of this essential amino acid at the initial rate-limiting step, IDO1 activity leads to the production of L-kynurenine (Kyn), which is the upstream metabolite along the so-called kynurenine pathway.[2] The enzymatic activity was the first and better characterized IDO1 feature and, by causing Trp starvation and Kyn production, it leads to the conversion of naïve $CD4^+$ T cells into regulatory T cells (Treg).[3] In addition, Kyn activates the aryl hydrocarbon receptor (AhR), whose signaling plays an important role in the immune system.[4,5]

Recently, the nonenzymatic function of IDO1, mediated by its heme-free form (apo-form), has been described as an additional tolerogenic mechanism (Figure 1B). IDO1, in a microenvironment dominated by immunoregulatory TGF-β, thanks to its two immunoreceptor tyrosine-based inhibitory motifs (ITIMs), upon tyrosine phosphorylation, recruits SHP's family tyrosine phosphatases and thus activates several signaling events that confer a long-term immunoregulatory phenotype in conventional DCs (cDCs) and plasmacytoid DCs (pDCs).[6,7] IDO1 is also endowed with a YxxM ("x" indicates any amino acid) phosphorylation motif, through

Received: May 3, 2024
Revised: July 20, 2024
Accepted: July 23, 2024
Published: September 12, 2024

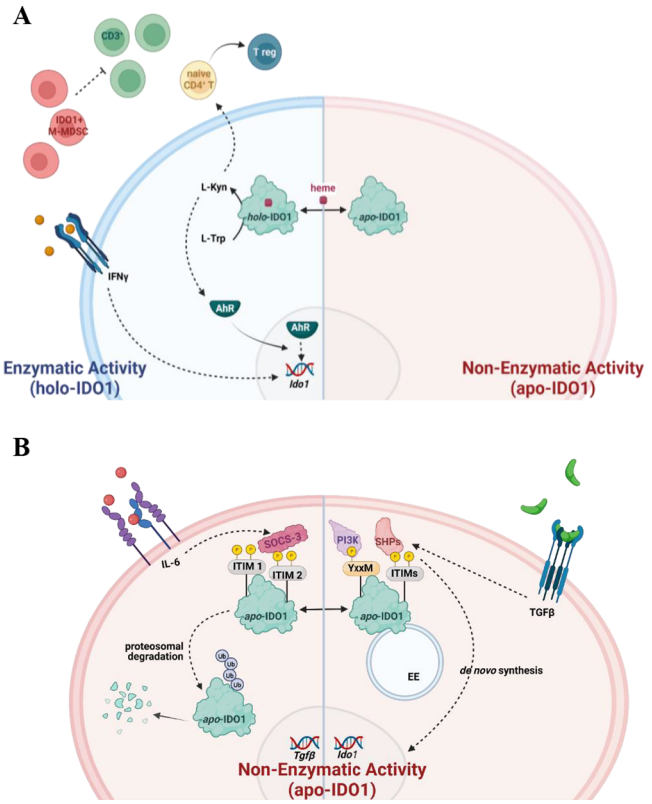

Figure 1. Enzymatic (A) and nonenzymatic (B) activities of IDO1.

which it can directly bind the class IA PI3K regulatory subunit and then anchor to early endosomes (EEs), which represent the subcellular localization specific for the IDO1-mediated signaling function.[8] Moreover, pro-inflammatory contexts driven by IL-6 are characterized by the upregulation of SOCS3, which associates with phosphorylated ITIM2 via its SH2 domain, recruits the E3 ubiquitin ligase complex, and directs cytosolic IDO1 to proteasomal degradation.[1] In cancer, the inducible or constitutive IDO1 expression correlates with a negative prognosis for patients, representing one of the critical tumor-escape mechanisms.[9] Therefore, several molecules have been developed to inhibit the catalytic activity and enhance antitumor immune responses.[10,11] Many preclinical data have demonstrated that inhibiting the IDO1 enzyme can empower the efficacy of cytotoxic chemotherapy, radiotherapy, and immune checkpoint therapy.[12] However, during clinical trials, epacadostat, a holo-IDO1 inhibitor, disappointed the expected antitumor efficacy.[13] Among the possible explanations for this negative result[14] is its inability to block the noncatalytic function of IDO1 or even to enhance it.[15] Our study was focused on finding a more efficient strategy for targeting IDO1. Here, we aim to characterize a small molecule that has an unprecedented profile, being capable of inhibiting both the enzymatic and nonenzymatic functions of IDO1 by binding to its apo-form.

RESULTS

Identification, Synthesis, and Characterization of a Novel Compound Binding to IDO1. To identify novel and effective IDO1 inhibitors, a structure-based virtual screening was performed.[16,17] As no apo-inhibitor at that time was known in the literature, we focused our attention on the holo-form of the enzyme (PDB id: 2D0T) and performed a molecular docking screening of a subset of the ZINC15 database using the software FRED.[18] The first 50 selected structures were purchased, and the screening was performed by using an MTT assay to assess cytotoxicity.[16,17] Noncytotoxic compounds up to 30 μM were further screened in a cell-based assay in A375 cells to select only cell-permeable IDO1 inhibitors. Inhibitory activity was assessed by quantifying the Kyn level upon the induction of IDO1 with IFN-γ. Compound VS-15 (Scheme 1) was identified as a hit compound of interest, with no cytotoxicity up to 30 μM (Figure S1), an IC_{50} value of 0.48 μM $\pm$ 0.02 μM (Figure S2), and chemical stability in different buffers (Figure S3). To validate our discovery, the hit compound was synthesized in our laboratory according to Scheme 1 and retested to confirm both its chemical identity and biological activity. As illustrated in Scheme 1, compound VS-15 was synthesized through a three-step process. Initially, anthranilic acid **1** underwent *N*-acylation, resulting in compound **3**. Subsequently, in the second step, a nucleophilic substitution occurred to produce intermediate **5**. This intermediate readily engaged in a coupling reaction with tryptamine, yielding the final compound as a white solid. More details are reported in the SI. The compound was retested under the same conditions, and its potency was in accordance with the commercially available compound.

Then, cell viability in P1 tumor cells stably transfected with human (P1.hIDO1) or mouse (P1.mIDO1) IDO1 was assessed, and a cytotoxic effect was observed starting from 15 μM (Figure S4). The IC_{50} values obtained from the cellular assay were in good agreement (0.58 $\pm$ 0.04 μM on human IDO1 and 0.58 $\pm$ 0.01 μM on mouse IDO1) with the results obtained in A375 (Figure 2A). The reduction in Kyn levels was

Scheme 1. Synthesis of VS-15[a]

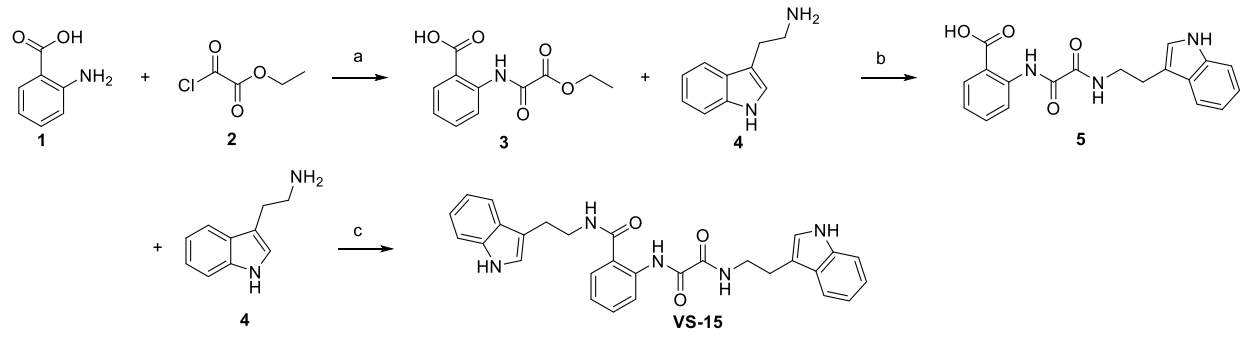

[a]Reaction conditions: (a) dry THF, 0°C; (b) toluene, TEA, reflux; (c) TEA, HOBt, EDC, dry DCM, rt.

https://doi.org/10.1021/acsptsci.4c00265
ACS Pharmacol. Transl. Sci. 2024, 7, 3056−3070

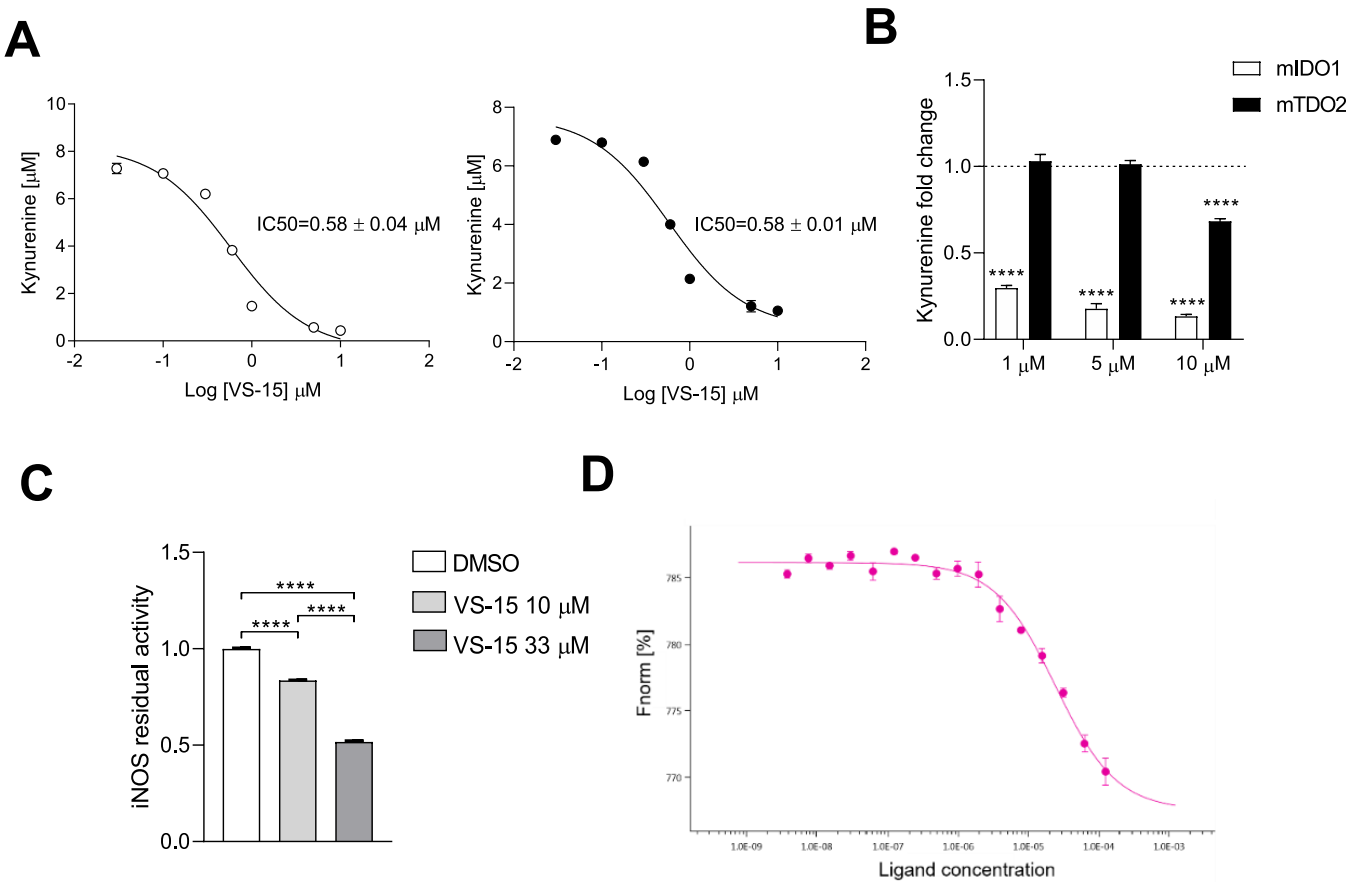

Figure 2. Identification and characterization of a novel compound binding to IDO1. (A) Cellular IC_{50} value (μM) of VS-15 obtained from a dose−response curve in P1 tumor cells stably transfected with human (left) or mouse (right) IDO1. (B) Kyn fold change in the supernatants from P1 tumor cells stably transfected with mouse IDO1 or TDO2 incubated with three different dilutions of VS-15 relative to the same cells treated with only the vehicle alone. (C) Residual activity of the iNOS enzyme expressed as a percentage of free enzyme activity that was defined as 100. (D) IDO1 MST binding curve in the presence of VS-15. The recombinant protein was mixed with a serial dilution of the compound starting at 250 μM to evaluate the binding of VS-15 to IDO1. In (A−D), results are the mean of three independent experiments, each performed in triplicate. Statistical analysis was performed using two-tailed paired Student's t test (B) or ANOVA followed by posthoc Bonferroni's test (C). ****p < 0.0001.

due to the inhibition of IDO1 catalytic activity and not due to the induction of IDO1 protein degradation by VS-15. Indeed, we have previously demonstrated that, when IDO1 associates with SOCS3 through its ITIM motifs, the enzyme can be triggered to proteasomal degradation.[19] Thus, we analyzed the kinetics of the intracellular protein degradation by a cycloheximide-chase assay followed by immunoblotting. We found that the turnover of the IDO1 protein in VS-15-treated cells overlapped the pattern observed in the control samples, indicating that this compound does not affect the ITIM-mediated mechanism of the proteasomal degradation of IDO1 (Figures 3 and S5).

To verify the selectivity of VS-15, we tested the molecule in P1 tumor cells stably expressing mouse tryptophan 2,3-dioxygenase (TDO), a closely related Trp-metabolizing enzyme. The cellular test demonstrated a dose-dependent inhibition of Kyn production by P1.IDO1, while in P1.TDO cells a weak effect was detected only at the highest nontoxic concentration of the compound (Figure 2B). Of note, in the literature VS-15 is described as an iNOS inhibitor based on the reduction of NO production in a cell-based assay.[20] Thus, the ability of the molecule to inhibit recombinant mouse iNOS was investigated by monitoring the oxidation of the NADPH cofactor.[21] VS-15 halves the NADPH oxidation rate only at a concentration of 33 μM, 100-fold higher compared with the IC_{50} value of IDO1 inhibition, pointing to VS-15 as a selective inhibitor of IDO1 over iNOS (Figure 2C). VS-15 binding to IDO1 was assessed by microscale thermophoresis (MST) experiments (Figure 2D) on recombinant human IDO1 (Figure S6), leading to a K_d value of 24.29 ± 3.76 μM.

Overall, our screening allowed us to identify and select VS-15, a small molecule that can effectively and selectively inhibit IDO1-mediated Kyn production in a cellular system.

VS-15 Is a Novel Inhibitor of Apo-IDO1. To investigate whether VS-15 could inhibit the apo-form of IDO1, we set up a spectrophotometric assay monitoring the loss in absorbance at the corresponding Soret maxima after the addition of VS-15.[22] We compared the off-rate of the heme cofactor in its ferric state in the presence and absence of the inhibitor, demonstrating that the kinetics of heme dissociation is fast as a result of the stabilization of the protein in its apo state by VS-15 (Figure 4A). Apo-IDO1 inhibition increases in a heme-reduced environment.[23] To reproduce this condition in cell-based assays, we treated cells with the heme biosynthesis inhibitor succinylacetone.[24] In this setting, the *de novo* synthesized IDO1 is produced in the presence of reduced levels of heme, it is expected to be mainly in its apo-form, and Kyn is produced only by the basal level of holo-IDO1. The

https://doi.org/10.1021/acsptsci.4c00265
ACS Pharmacol. Transl. Sci. 2024, 7, 3056−3070

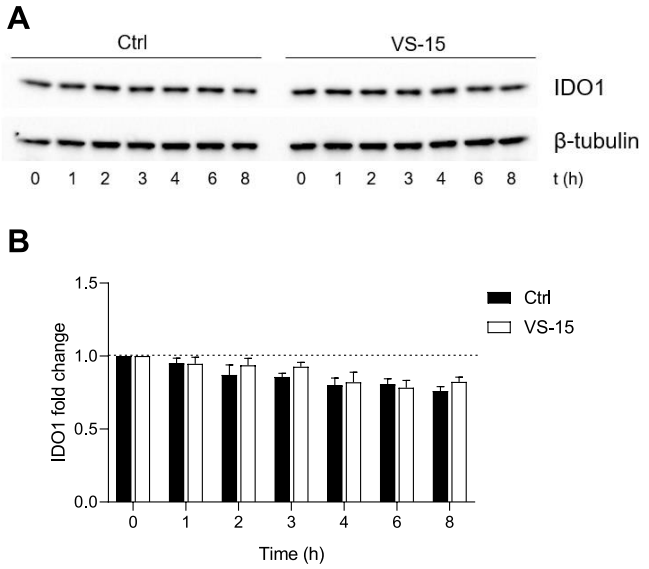

Figure 3. VS-15 does not affect IDO1 protein degradation. (A) Cycloheximide-chase assay followed by immunoblot analysis of IDO1 protein expression in lysates from P1.IDO1 cells pretreated with cycloheximide for 1 h and then exposed to VS-15 (1 μM) for the indicated time (from 0 to 8 h). For each time point, vehicle-treated cells were used as a control (Ctrl). β-tubulin expression was used as a normalizer. One representative experiment is shown. (B) Quantitative analysis of three independent experiments (mean ± SD) of Western blot analysis is represented as the fold change of normalized IDO1 protein at each time point over time 0. No statistically significant differences were determined between VS-15-treated and untreated samples.

Kyn level was lower in the presence of succinylacetone at all tested concentrations, inducing a shift in the concentration/response curve for VS-15 (Figure 4B). The calculated IC_{50} value under these conditions was 0.27 ± 0.015 μM (versus 0.48 μM under physiological conditions).

Peculiar settings are required to detect the effect of inhibitors of the apo-form of IDO1 by biochemical assays.[25] Therefore, the assay on the recombinant IDO1 protein was performed under different conditions of preincubation duration and temperature (Figure 4C,D). VS-15 inhibited the enzymatic activity of IDO1 only under forced conditions (Figure 4D), consistent with the behavior of an apo-IDO1 inhibitor. Conversely, epacadostat, a heme-coordinating compound used as a control, exerted its inhibitory effect under both experimental conditions used, but with a minimal change in its potency and comparably to the data reported in the literature.[25] By quantifying the free heme released after the incubation of rhIDO1 with the compound, a significant increase in free heme relative to the vehicle was seen, suggesting that VS-15 displaces heme from IDO1 upon binding, probably following a competition for the same site (Figure 4E). As previously described, epacadostat did not lead to the loss of heme by the IDO1 protein.[25] Moreover, in an experimental setting focused on the transition of the enzyme in its apo-form, VS-15 drives the dissociation of the cofactor with a K_d value of 63 μM (Supporting Information, Table 1), which is in good agreement with the affinity parameters calculated by MST (Figure 2D). Interestingly, the plot of the rates of displacement as a function of VS-15 concentration revealed a sigmoidal response that has been fitted with the Hill–Langmuir equation (Figure 4F). The goodness of fitting parameters and the value of the Hill coefficient (h = 2.41) suggest that IDO1 undergoes homotropic allosteric regulation by VS-15.

To investigate the VS-15 binding mode, a docking study was performed[26,27] using an X-ray crystal structure of apo-IDO1 (PDB id: 6MQ6, chain B). VS-15 pose was simulated using FRED software[18] after conformer generation with the software OMEGA2,[26,27] and the docking procedure was designed in accordance with our previous virtual screening on IDO1.[16,17] The resulting pose (Figure 5) revealed that the central aromatic ring of VS-15 is accommodated in pocket A (Tyr126, Cys129, Val130, Phe163, Phe164, Ser167, and Ala264), while the indole group interacts with Phe163 with a $\pi-\pi$ interaction. This indole moiety is also located in proximity to Phe226 of pocket B (Phe226, Arg231, Ile232, Leu234, and Ser235). Furthermore, a hydrogen bonding interaction occurs between a carbonyl oxygen of the amide group and Ser167. Pocket C (Lys238, Ala260, Gly261, Gly262, Ser263, and Phe291) is not exploited except for hydrophobic contact with Ser263. In agreement with the pose of previously identified apo-IDO1 inhibitors,[28] the other indole group of VS-15 extends into pocket D (Val170, Ser267, Val269, Phe270, Leu359, Leu342, Arg343, and His346), where it can give a hydrogen bonding interaction with Ser267 and a hydrophobic interaction with the side chains of the other amino acids.

As a whole, these data reveal that VS-15 is an inhibitor of apo-IDO1.

VS-15 Negatively Regulates IDO1-Mediated Signaling. Besides catalytic activity, IDO1 is endowed with a signaling function[6] and the two activities are spatially segregated.[8] To investigate whether VS-15 may interfere with IDO1-mediated signaling function, we first evaluated IDO1-p85 binding. Coimmunoprecipitation experiments revealed that PI3K p85 subunit binding to IDO1 is reduced in the presence of the compound (Figures 6A and S5). As a result, VS-15 significantly and strongly impairs the IDO1 localization in the subcellular compartment that allows IDO1 signaling function, namely, EEs, by retaining the protein in the cytosol (Figures 6B–C and S5). The IDO1 nonenzymatic function depends on its association with tyrosine phosphatases SHPs.[6,8] A coimmunoprecipitation assay performed as in Figure 6A showed that VS-15 causes a strong reduction of both SHP-1 and SHP-2 binding to IDO1 (Figures 6D and S5). This finding was confirmed by the evaluation of the ability of IDO1 immunoprecipitates to remove a phosphate group from a tyrosine-phosphorylated substrate, as previously described.[6] Preconditioning of the cells with VS-15 significantly reduced the level of free phosphate, as compared with the control (Figure 6E).

The IDO1-mediated signaling function was first described in pDCs,[6] and TGF-β induces IDO1-dependent immunoregulatory effects in pDCs *in vivo* relying on the ITIM-mediated signaling activity of the protein.[1,29] To investigate whether VS-15 could affect the TGF-β-mediated immunosuppressive function in pDCs, we used a skin test assay, which represents a consistent tool for discriminating between the immunogenic and immunosuppressive potential of distinct DC subsets conditioned with different stimuli.[6,19,30] As expected, the default priming ability of immunostimulatory $CD8^-$ DCs was suppressed by the TGF-β-treated pDCs,[6] while VS-15 abrogated the immunosuppressive response elicited by the cytokine (Figure 7).

https://doi.org/10.1021/acsptsci.4c00265
ACS Pharmacol. Transl. Sci. 2024, 7, 3056–3070

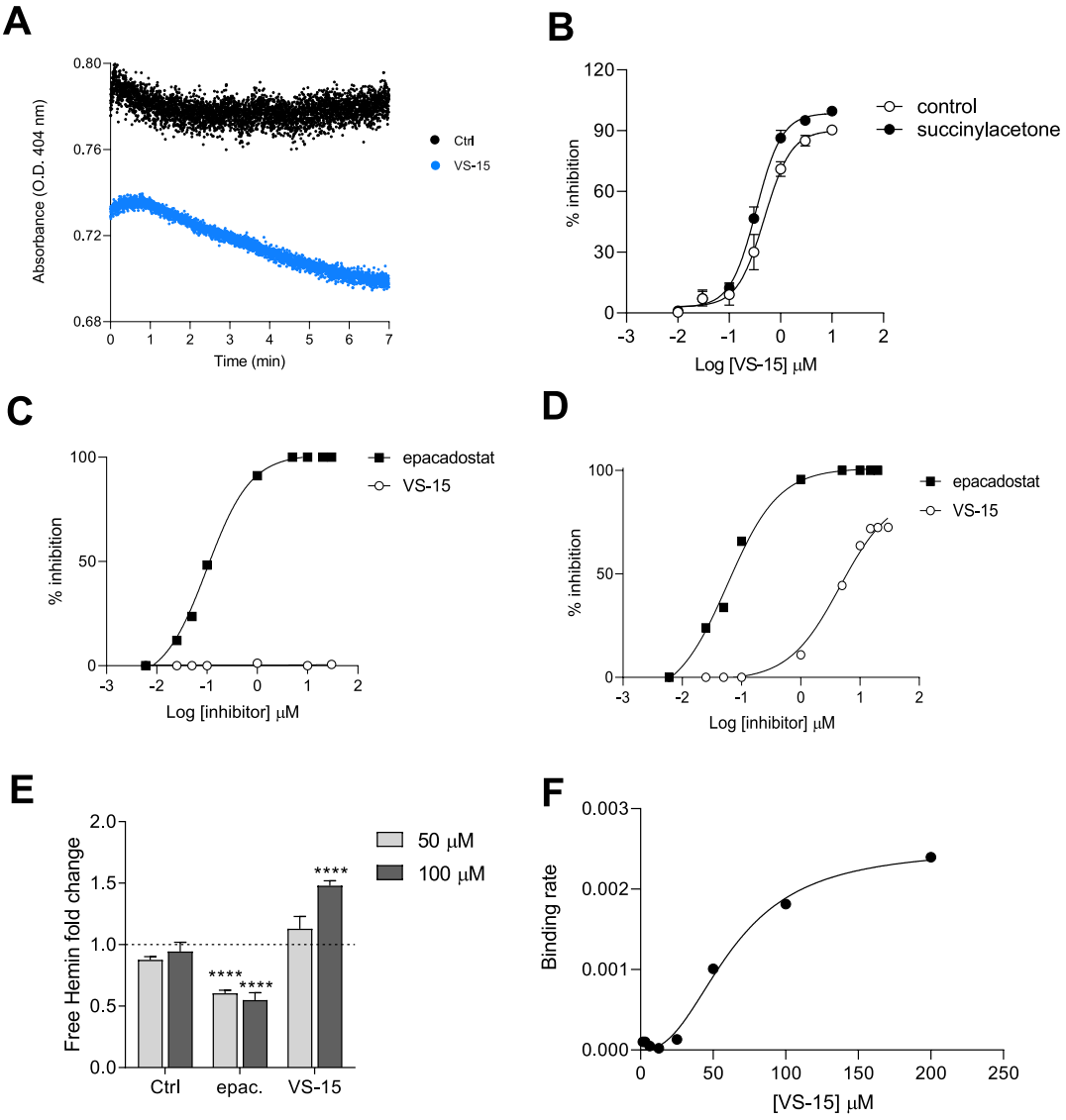

Figure 4. VS-15 is an inhibitor of apo-IDO1. (A) Absorbance-based tracking of the displacement of heme from IDO1. The loss of absorbance at the IDO1 λ_{max} of the Soret peak (404 nm) has been evaluated as a function of time in the absence (black) and the presence (blue) of 10 μM VS-15 inhibitor. (B) Inhibition profile of VS-15 in A375 cells stimulated with IFN-γ in the presence or absence of succinylacetone, tryptophan, and increasing concentrations of VS-15 for 48 h. Each experiment included the corresponding controls: IFN-γ treatment alone for the standard assay and IFN-γ plus succinylacetone treatment. The IC_{50} value under physiological conditions (control) was 0.48 μM, while with succinylacetone treatment it was 0.27 μM. (C) Inhibition profile of VS-15 and epacadostat (epac.) (relative to the DMSO control) in the hIDO1 biochemical assay performed under standard conditions. The epacadostat IC_{50} value was 0.01 μM. (D) Inhibition profile of VS-15 and epacadostat (epac.) (relative to the DMSO control) in the hIDO1 biochemical assay performed at increased preincubation time and temperature. Under these conditions, the IC_{50} value was 0.05 μM for epacadostat and 4.6 μM for VS-15. (E) Free heme release after incubation of hIDO1 with two different concentrations of VS-15, epacadostat, or DMSO as a control (Ctrl). Data are presented relative to the untreated sample (dotted line, 1-fold). ****$p < 0.0001$ (paired Student's t test). (F) Binding affinity of VS-15 defined as a result of the heme dissociation rate at different inhibitor concentrations (K_d = 63 μM). In (B–E), data are the mean ± SD of three independent experiments, each performed in triplicate.

Moreover, VS-15 significantly opposed the TGF-β immunosuppressive effects mediated by IDO1 signaling, namely the downstream induction of TGF-β and IDO1 themselves (Figures 8A,B and S5).

In addition, the tyrosine-phosphatase activity in IDO1 coimmunoprecipitates from pDCs treated with TGF-β was markedly suppressed by treatment with VS-15 before treatment with TGF-β (Figures 8C and S5).

In conclusion, in pDCs, VS-15 counteracts TGF-β-mediated activation of the positive immunoregulatory circuitry that involves the IDO1 signaling pathway.

VS-15 Abrogates the Immunosuppressive Function of Tumor Patient-Derived Circulating Monocytes. During tumor progression, cancer cells release several pro-inflammatory molecules that trigger the expansion and accumulation of alternative monocytes named monocytic myeloid-derived suppressor cells (M-MDSCs), which promote several immune escape mechanisms exploited by cancer.[31,32] Among these, M-MDSCs inhibit T cell-mediated immune responses through various mechanisms, including their ability to proliferate and trigger an efficient antitumor response.[33] To investigate the clinical potential of VS-15, we tested if it could inhibit the immunosuppressive activity of circulating M-

https://doi.org/10.1021/acsptsci.4c00265
ACS Pharmacol. Transl. Sci. 2024, 7, 3056−3070

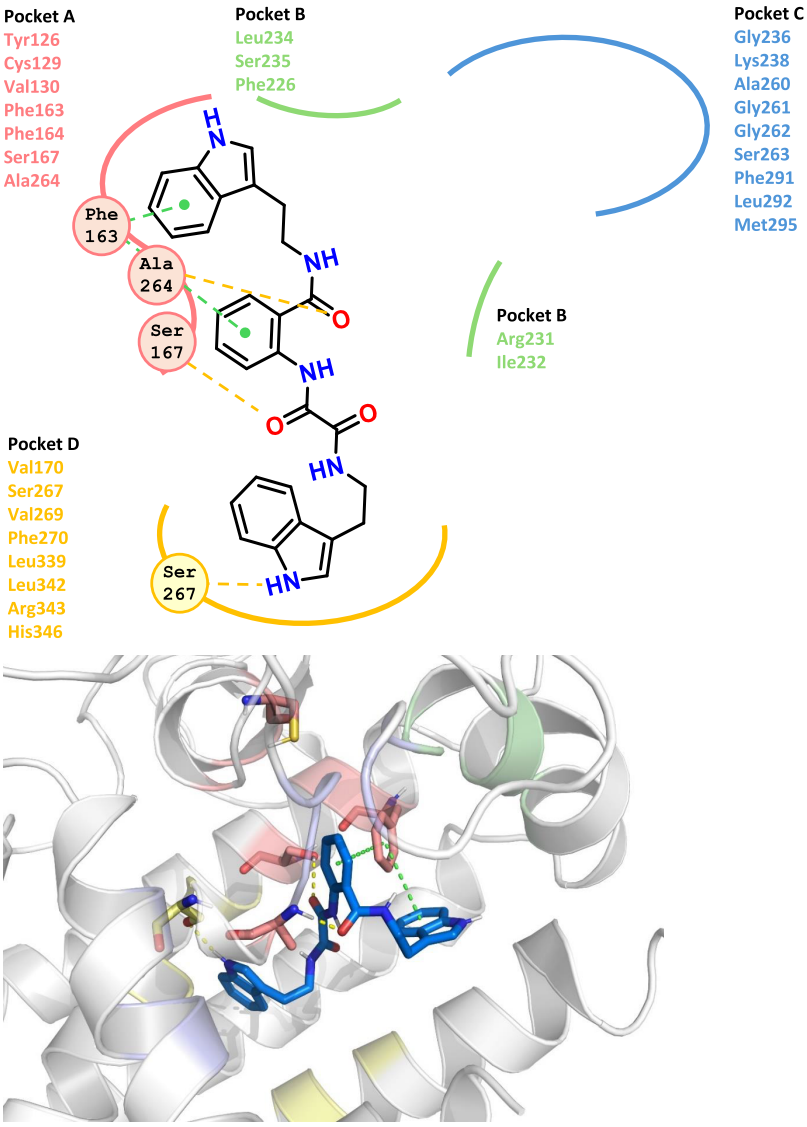

Figure 5. Docking pose of VS-15 in apo-IDO1. Location of the binding region on the IDO1 crystal structure (PDB id: 6MQ6) and docking pose of compound VS-15, depicted as blue sticks. The central aromatic ring of VS-15 is situated within pocket A (red) (Tyr126, Cys129, Val130, Phe163, Phe164, Ser167, and Ala264). The indole group interacts with Phe163 with a $\pi-\pi$ interaction and is also located in a hydrophobic subpocket in the proximity of Phe226 in pocket B (green) (Phe226, Arg231, Ile232, Leu234, and Ser235). Furthermore, hydrogen bonding interactions occur between a carbonyl oxygen of the bicarbonyl moiety and Ser167 and also between another carbonyl oxygen and Ala264. Pocket C (blue) is not exploited, except for hydrophobic contact with Ser263. The other indole group is located in pocket D (yellow) (Val170, Ser267, Val269, Phe270, Leu359, Leu342, Arg343, and His346), where it forms a hydrogen bonding interaction with Ser267 and engages in hydrophobic interactions with the side chains of surrounding other amino acids (Val170, Leu342, and Phe270).

MDSCs from patients affected by different types of cancer, i.e., breast (BC), pancreatic (PC), and lung (LC) cancer. To assess the involvement of IDO1 in the pro-tumoral activity mediated by M-MDSCs, we first evaluated by flow cytometry the expression of IDO1 in circulating monocytes from PC, BC, and LC patients in comparison to HD (Figure 9A). The percentage of IDO1$^+$ monocytes was strongly variable among patients affected by different types of tumors, the PC patients having the highest percentage of IDO1$^+$ monocytes, while in BC patients it was similar to HD (Figure 9B). As the presence of IDO1$^+$ monocytes in LC was frequently undetectable and significantly lower compared to HD, we did not take into account LC patients for subsequent analyses. IDO1-expressing monocytes showed a low level of HLA-DR, resembling conventional M-MDSCs (CD14$^+$HLA-DR$^{low/-}$), compared to the IDO1 negative monocyte counterpart (Figure S7).

To study the role of IDO1 in mediating M-MDSCs' immunosuppressive activity, the percentage of IDO1$^+$ monocytes observed in the peripheral blood of BC and PC patients was correlated with the capacity to restrict the proliferation of activated T cells (Figure 9C). Interestingly, we observed a significant indirect correlation between the IDO1 expression in monocytes isolated from patients and their ability to suppress the *in vitro* proliferation of activated CD3$^+$ T lymphocytes (Figure 9C), suggesting a critical role of IDO1 expression in driving the immunosuppressive functions of monocytes from tumor patients. As previously shown,[31,33] circulating monocytes isolated from tumor patients can be divided into two distinct subgroups: "suppressive monocytes" (which resemble M-MDSCs), able to reduce T cell proliferation, and "nonsuppressive monocytes", which do not inhibit T cell proliferation, similarly to the healthy donor

https://doi.org/10.1021/acsptsci.4c00265
ACS Pharmacol. Transl. Sci. 2024, 7, 3056−3070

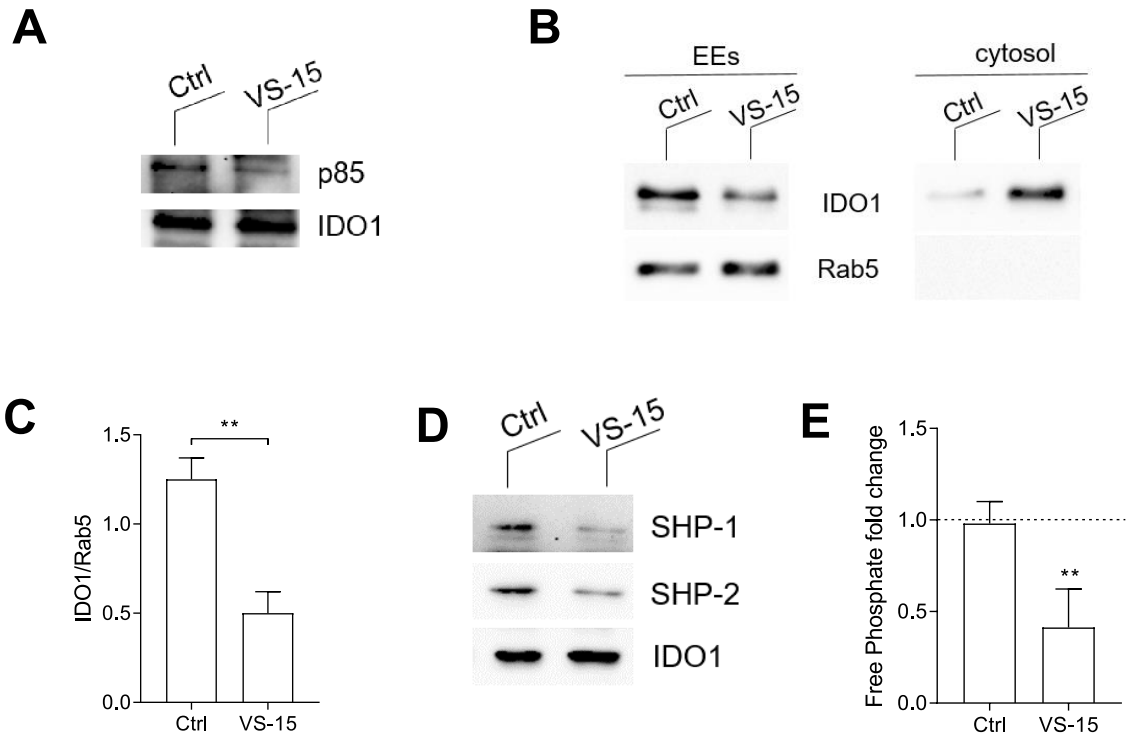

Figure 6. VS-15 negatively regulates IDO1-mediated signaling events in P1 tumor cells overexpressing IDO1. (A) Immunoprecipitation of IDO1 from P1.IDO1 cells treated with VS-15 (1 μM) or the vehicle alone (Ctrl) and detection of IDO1 or p85 PI3K by sequential immunoblotting. (B) Immunoblot analysis of endosome (EEs) and cytosol isolated from VS-15-treated P1.IDO1 cells. Cells incubated with the vehicle DMSO were used as a control (Ctrl). (C) Quantitative analysis of three independent immunoblot experiments, one of which is represented in (B). The IDO1:Rab5 ratio was calculated by densitometric quantification of the specific bands. (D) Immunoblot analysis of coimmunoprecipitates from P1.IDO1 cells treated as in (A). (E) Phosphatase activity produced by IDO1 immunoprecipitated from P1.IDO1 cells treated as in (A). Levels of free phosphate (pmol) generated during the incubation of a tyrosine-phosphorylated peptide with the coimmunoprecipitated IDO1 proteins from each condition were presented as a fold change relative to untreated cells (dotted line, 1-fold). In (A, B, D), one experiment representative of three is shown. In (C, E), results are representative of three independent experiments (mean ± SD), each performed in triplicate. In (C, E), $^{**}p < 0.01$ (paired Student's t test).

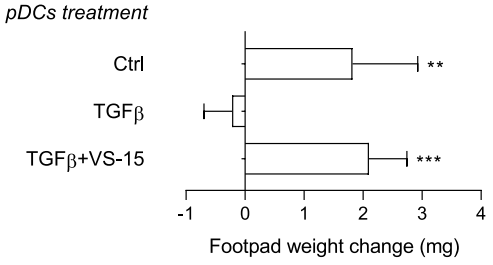

Figure 7. VS-15 abrogates the TGF-β-dependent tolerogenic response in pDCs *in vivo*. Skin test reactivity of mice sensitized with splenic HY-pulsed immunostimulatory cDCs combined with a minority fraction (5%, indicated) of pDCs. pDCs were conditioned *in vitro* with the vehicle DMSO (Ctrl) or TGF-β, in the presence or absence of VS-15 (1 μM), before being HY-pulsed together with the cDC majority fraction and i.p. transferred into syngeneic C57BL/6 recipient female mice. Analysis of skin reactivity of recipient mice to the eliciting peptide at 15 days is presented as a change in footpad weight (experimental versus control footpads). $^{**}p < 0.01$ and $^{***}p < 0.001$ (Tukey's multiple comparison test).

(HD)-derived monocytes. To evaluate the capability of VS-15 to reduce the MDSC-dependent immunosuppressive activity, we first tested its toxicity in monocytes isolated from HD (Figure 9D). Then, the viability of BC and PC patient-derived monocytes treated with VS-15 at 1 μM, i.e., the concentration used for the biochemical and cell-based assays, was assessed (Figure 9E). The study of the ability of VS-15 to restrict the pro-tumoral functions of tumor patient-derived monocytes revealed that the compound significantly reduces the capacity of "suppressive monocytes" to inhibit T cell proliferation (Figure 9F). As expected, VS-15 was ineffective on non-suppressive tumor patient-isolated monocytes (Figure 9F).

Overall, these results corroborate not only the impact of IDO1 in driving the inhibitory function of tumor-isolated immunosuppressive monocytes but also the substantial clinical potential of the novel compound VS-15 for limiting the mechanisms of immune escape mediated by cancer.

DISCUSSION

Great interest in the study of IDO1 as a target in cancer derives from the finding that approximately 50% of human tumors express IDO1.[9] The ability of this enzyme to catalyze the degradation of the essential amino acid Trp together with the production of the immunosuppressive Kyn has pointed to IDO1 as an immune checkpoint molecule with a key role in cancer evasion of immune responses.[34,35] However, several discoveries have changed the perspectives on this enzyme over the last decades.

First, negative clinical results were reported on IDO1 small-molecule inhibitors developed to block its catalytic activity, which were effective in multiple preclinical tumor models. In particular, the large phase III combination trial of epacadostat in combination with the reference pembrolizumab therapy in advanced melanoma patients failed to show a clinical benefit

https://doi.org/10.1021/acsptsci.4c00265
ACS Pharmacol. Transl. Sci. 2024, 7, 3056−3070

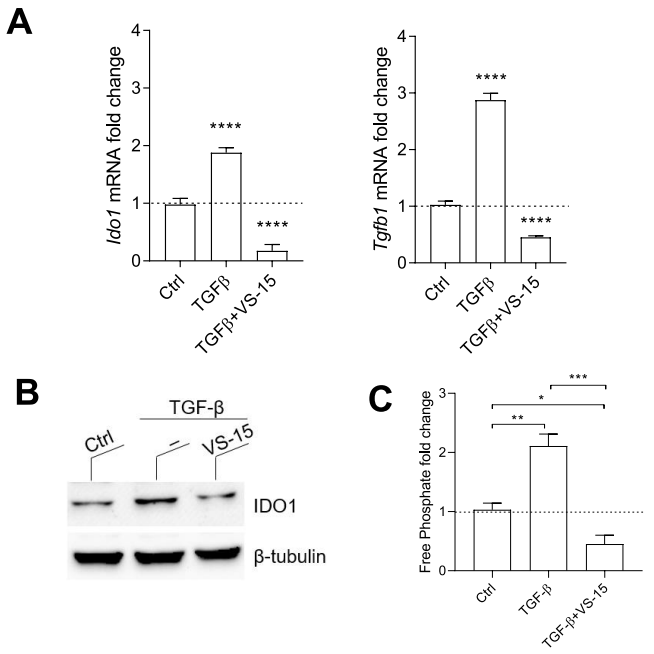

Figure 8. VS-15 negatively regulates IDO1-mediated signaling events in pDCs. (A) Real-time PCR analysis of *Ido1* and *Tgfb1* transcripts in pDCs treated with TGF-β alone or in combination with VS-15 (1 μM) or the vehicle as a control (Ctrl). Transcript expression was normalized to the expression of *Gapdh* and presented relative to results in untreated cells (dotted line, 1-fold). Results are representative of three independent experiments (mean ± SD), each performed in triplicate. (B) Immunoblot analysis of IDO1 protein expression in lysates from pDCs cells treated as in (A). β-Tubulin expression was used as a normalizer. One representative immunoblot of three is shown. (C) Phosphatase activity produced by IDO1 immunoprecipitated from pDCs treated as in (A). Levels of free phosphate (pmol) generated during the incubation of a tyrosine-phosphorylated peptide with the coimmunoprecipitated IDO1 proteins from each condition were presented as a fold change relative to untreated cells (dotted line, 1-fold). In (A, C), results are representative of three independent experiments (mean ± SD), each performed in triplicate. *$p < 0.05$, **$p < 0.01$, ***$p < 0.001$, and ****$p < 0.0001$. In (A) paired Student's t test and in (C) one-way ANOVA followed by posthoc Bonferroni's test.

and, consequently, other trials have been suspended, canceled, or downsized.[36] These unexpected results, while dampening enthusiasm for the development of IDO1 inhibitors, raised new questions and stimulated further research for a deeper understanding of IDO1 biology[14,15] as well as for the discovery of new clinically effective inhibitors.

Second, IDO1 exists in a dynamic equilibrium between two alternative forms, a heme-bound form (holo-IDO1), which is catalytically competent, and a heme-free form (apo-IDO1), whose biology and functions are still under investigation.[22] Apo-IDO1 was detected and quantified in both tumor and nontumor cells, and it was suggested that apo/holo IDO1 balance could be cell-specific.[22,37] The discovery that IDO1 can also exist without heme has initiated the development of next-generation compounds,[22] named heme-displacing inhibitors. Among them, linrodostat mesylate (BMS-986205) reverted the immunosuppression in cancer patients by inhibiting IDO1 and decreasing the Kyn levels of tumor cells and is under evaluation in various trials.[38] Recently, it has been suggested that IDO1 apo-form can have an active role in tumor progression independently of the catalytic activity, but the underlying molecular mechanisms have not been explored yet.[39]

Third, IDO1 acts as a signal-transducing molecule capable of modulating immune responses independently of its catalytic activity.[1,6,8] It was demonstrated in DCs that under conditions favoring signaling, IDO1 interacts with class IA PI3Ks p85, shifts from the cytosol to EEs, and leads to the activation of IDO1-SHPs-mediated events, which culminate in the establishment of a sustained immunosuppressive pathway. However, the expression patterns of IDO1 in human cancer are complex and heterogeneous in different cells, namely, malignant, immune, stromal, and vascular within the tumor microenvironment and APCs. In addition, we have recently identified that IDO1-mediated signaling events can also occur in tumor cells, highlighting that the specific molecular mechanisms can be tumor-specific.[40] The nonenzymatic role of IDO1 in tumor progression independently of the catalytic activity[39,40] is also suggested by the ineffectiveness of the current generation of IDO1 enzyme inhibitors in reversing the IDO1-mediated immunosuppressive effects in DCs and tumor cells, with particular reference to the aging process.[15,41,42]

In this scenario, our study focused on finding a more efficient way of blocking IDO1 by searching for a small molecule capable of inhibiting its enzymatic and nonenzymatic functions. By virtual screening, we identified VS-15, which was profiled in various biochemical and cell-based assays. Although first described as an iNOS inhibitor, VS-15 showed strong IDO1 binding activity and ability to selectively inhibit this enzyme, rather than the enzymes TDO or iNOS. We demonstrated with different experimental approaches that VS-15 is capable of binding the apo-form of IDO1 and inhibiting its enzymatic activity. In this setting, it is possible to speculate that by binding and inhibiting the apo-conformation of IDO1, VS-15 subtracts the apo-form from equilibrium and therefore induces holo-IDO1 to change conformation to restore the equilibrium. Consequently, VS-15 can emerge as a crucial factor among the different elements influencing the levels of the two forms of the protein. This could happen independently of the specific apo/holo IDO1 present in the cell type.

Furthermore, the compound counteracts the events of the IDO1-mediated signaling pathway responsible for the establishment of the sustained immunosuppressive phenotype in cells. Indeed, in tumor cells overexpressing IDO1, the compound reduced the first events activating the IDO1-mediated signaling pathway, i.e., IDO1 binding to the PI3K regulatory subunit p85, to the tyrosine phosphatases SHPs as well as the IDO1 anchoring to the EEs. In pDCs, VS-15 counteracts the TGF-β-dependent IDO1-mediated signaling events, i.e., IDO1 interaction with tyrosine phosphatases and the self-maintaining regulatory circuitry by reducing the gene transcription of key molecules (*Ido1* and *Tgfb1*) and abrogating *in vivo* the TGF-β-mediated immunosuppressive phenotype in pDCs.

Overall, these findings point to VS-15 as a new immune checkpoint inhibitor targeting IDO1. To explore this hypothesis further, we investigated its ability to inhibit the immunosuppressive activity of circulating monocytes from patients affected by different types of cancer. Interestingly, in our study, we found different percentages of IDO1$^+$ monocytes in patients with different types of tumors, and pancreatic cancer is the one with the highest percentage of IDO1$^+$ cells. This finding confirms that IDO1 inhibition might not be useful

https://doi.org/10.1021/acsptsci.4c00265
ACS Pharmacol. Transl. Sci. 2024, 7, 3056−3070

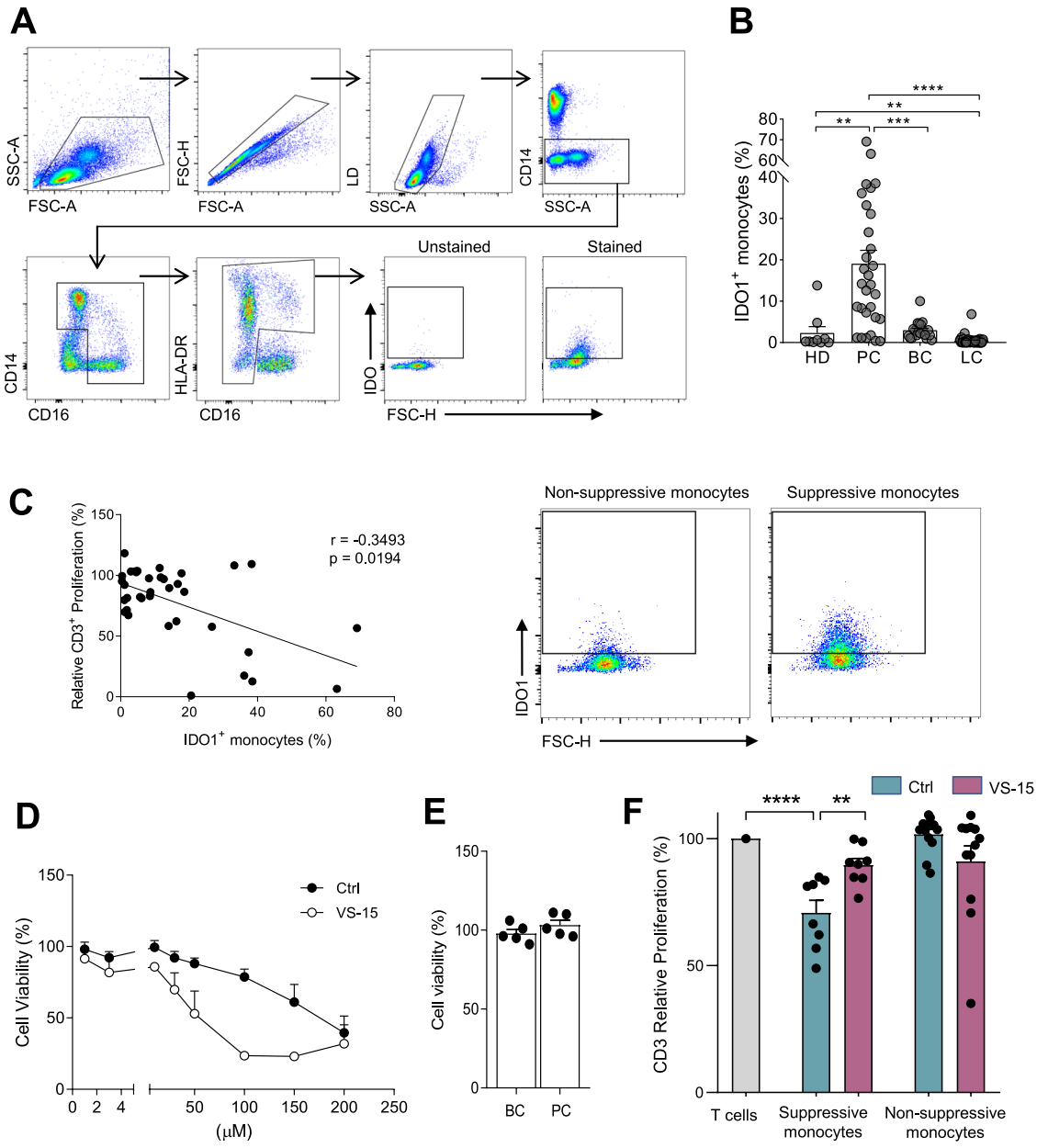

Figure 9. VS-15 abrogates the immunosuppressive function of circulating monocytes isolated from tumor patients in controlling T cell proliferation. (A) Representative gating strategy to evaluate the percentage of circulating IDO1$^+$ monocytes in the healthy donor (HD), pancreatic cancer (PC), breast cancer (BC), and lung cancer (LC) patients by flow cytometry. (B) Percentage of circulating IDO1$^+$ monocytes (out of total monocytes) in HD (n = 9), PC (n = 30), BC (n = 20), and LC (n = 45) patients. (C) Correlation between the percentage of PC- and BC-derived circulating IDO1$^+$ monocytes and the proliferation of activated CD3$^+$ T lymphocytes following the coculture with PC- and BC-derived monocytes (n = 36). Representative percentage of IDO1$^+$ monocytes analyzed by flow cytometry related to nonsuppressive and suppressive total monocytes derived from tumor patients is shown in the right panel. (D) Viability of HD-derived monocytes (n = 3) after 24 h treatment with different concentrations of VS-15 and DMSO as a control. (E) Viability of BC- and PC-derived monocytes (n = 5) after 24 h treatment with VS-15 at 1 μM. All values are normalized on cells treated with DMSO as a vehicle. (F) Relative proliferation percentage of CD3$^+$ T cells after 4 days of coculture with either suppressive (PC, n = 3; BC, n = 5) or nonsuppressive (PC, n = 6; BC, n = 6) monocytes pretreated with 1 μM of VS-15 and DMSO as a control. All values are normalized on activated T cells in the absence of myeloid cells. Data are expressed as mean ± SEM. $^{**}p < 0.01$, $^{***}p < 0.001$, and $^{****}p < 0.0001$. In (B) unpaired Student's t test and in (F) Wilcoxon's signed-rank test.

as a therapeutic approach in all oncological patients, a feature that should be taken into account in the design of clinical trials that assess the efficacy of IDO1 inhibitors. Monocytes from patients affected by pancreatic cancer were therefore used to evaluate the effect of VS-15: the compound significantly reduced the capacity of suppressive monocytes to inhibit T cell proliferation but was ineffective on nonsuppressive monocytes.

An alternative strategy to simultaneously inhibit both enzyme-mediated and nonenzyme-mediated functions of IDO1 is protein degradation through PROTACs, as exemplified by Bollu et al.[43] IDO1 degradation might be a more effective strategy to eliminate all activities associated with IDO1, but limitations in terms of druglikeness might hamper PROTAC development in the clinic. Hence, we postulate that negative modulators of IDO1 signaling activities represent a

https://doi.org/10.1021/acsptsci.4c00265
ACS Pharmacol. Transl. Sci. 2024, 7, 3056−3070

complementary option to be explored for several reasons. They behave as chemical probes for more precise control of the IDO1 partnership with PI3Ks and SHPs, offering a tool to better elucidate IDO1 biology. In addition, they offer an alternative approach to interfere with IDO1 signaling activities that might be easier to translate in the clinic, thanks to the low molecular weight of this small compound. In the future, it might be interesting to compare in *in vivo* studies the efficacy of our modulator with that of PROTACs and better understand the pros and cons of these two approaches.

In conclusion, we have discovered an IDO1 inhibitor that, thanks to its peculiar profile, might lay the basis for the development of a novel class of small molecules capable of blocking both the enzymatic and nonenzymatic functions of this moonlighting protein and improving the effectiveness of cancer immunotherapy.

METHODS

Animals and Reagents. C57BL/6 mice (6−8 weeks old, female, 15−20 g) were purchased from Charles River Breeding Laboratories Italia (Milan, Italy). All animals were housed and fed under specific pathogen-free conditions in the animal facility of the University of Perugia. All *in vivo* studies were compliant with National (Italian Animal Welfare Assurance A-3143-01) and Perugia University Animal Care and Use Committee guidelines. DMSO was purchased from Sigma-Aldrich (MO, USA). The H-2Db-restricted HY peptide (WMHHNMDLI), containing the immunodominant epitope of male mouse-specific minor transplantation antigen, was synthesized by BioFab Research (Rome, Italy). Recombinant mouse iNOS was purchased from Sigma-Aldrich N2783−50UN. Epacadostat was purchased from Selleckchem (Huston, TX, USA), and the other reagents for the preparation of VS-15 were purchased from Sigma-Aldrich (MO, USA), TCI Europe (Zwijndrecht, Belgium), and BLD-Pharm (Hamburg, Germany).

Cell Lines and Cell Culture. Cells of P1.HTR, a highly transfectable clonal variant of mouse mastocytoma P815,[44] were transfected by electroporation with a plasmid construct coding for mouse (P1.mIDO1), human (P1.hIDO1) IDO1 or for mouse TDO2 (P1.TDO2) as described in previous works.[6,45] The stable transfectant cell line was obtained by puromycin selection and cultured in Iscove's modified Dulbecco's medium (Gibco, Invitrogen CA, USA) supplemented with 10% FCS (Gibco, Invitrogen CA, USA), 1 mM glutamine (Gibco, Invitrogen CA, USA), and penicillin/streptomycin (Gibco, Invitrogen CA, USA) at 37 °C in a humidified 7% CO_2 incubator. A375 cells were grown with RPMI supplemented with 10% fetal bovine serum (FBS), 2 mM L-glutamine, 100 U/mL penicillin, and 100 mg/mL streptomycin (GE Healthcare, Milan, Italy). In every cellular assay, the cell line was used at a passage number not exceeding the 10th.

Human Primary Cell Culture. Peripheral blood samples were collected from different tumor patients (PC, pancreatic cancer n = 30; BC, breast cancer n = 20; LC, lung cancer n = 45) in the Oncology Unit of the Azienda Ospedaliera Universitaria Integrata Verona or from healthy donors (HD, n = 9). No subject was undergoing therapy at the time of sample collection. Peripheral blood mononuclear cells (PBMCs) were isolated by a Ficoll-Hypaque (GE Healthcare). Monocytes were isolated from PBMCs by using CD14 MicroBeads (Miltenyi Biotec) according to the manufacturer's instructions with at least 95% cell purity, as evaluated by flow cytometry. Cells were cultured in a humidified atmosphere (5% CO_2, 37 °C). This study was approved by the local ethical committee (Prot. 51095, 19/07/2018; Prot. 17963, 25/03/2020) and conducted according to the Declaration of Helsinki and Good Clinical Practice.

Concentration−Response Curve of VS-15. The concentration−response curve for extrapolating the IC_{50} (half-maximal inhibitory concentration) value of VS-15 in P1.IDO1 cells was obtained through a cellular assay by incubating cells with 2-fold serial dilutions of the compound. After incubation, supernatants of cell cultures were recovered, and the Kyn concentration was detected by HPLC. The control was represented by cells incubated with an equivalent volume of DMSO, the vehicle in which VS-15 was solubilized.

Kynurenine Measurements. Detection of Kyn concentrations was performed using a PerkinElmer, series 200 HPLC instrument (MA, USA). A Kinetex C18 column (250 × 4.6 mm, 5 μm, 100 Å; Phenomenex, USA), maintained at the temperature of 25 °C and pressure of 1800 PSI, was used. A sample volume of 300 μL was injected and eluted by a mobile phase containing 10 mM NaH_2PO_4 pH 3.0 (99%) and methanol (1%) (Sigma-Aldrich, MO, USA), with a flow rate of 1 mL/min. Kynurenine was detected at 360 nm with a UV detector. The software TURBOCHROM 4 was used for evaluating the concentration of kynurenine in samples using a calibration curve. The detection limit of the analysis was 0.05 μM.

Microscale Thermophoresis (MST). Experiments to assess K_d values were conducted by using a Monolith NT.115 instrument (NanoTemper Technologies, Munich, Germany). Fluorescence labeling of rhIDO1 was performed following the protocol for the *N*-hydroxysuccinimide (NHS) coupling of RED dye NT650 (NanoTemper Technologies, Munich, Germany) to lysine residues. Briefly, 100 μL of a 20 μM solution of rhIDO1 protein in MES buffer (25 mM MES, 150 mM KCl, pH 6.5) was mixed with 100 μL of 80 μM NT650-NHS fluorophore (NanoTemper Technologies, Munich, Germany) and incubated for 30 min at room temperature in the dark. Unbounded fluorophores were removed by size-exclusion chromatography with MST buffer (50 mM TRIS, 150 mM NaCl, 10 mM $MgCl_2$, pH 7.4, 0.05% Tween20) as the running buffer. The real concentration of each element of the sample, such as protein, heme group, and RED dye, and the degree of labeling (DoL) were determined using the extinction coefficients ε_{280} = 51,380 M^{-1} cm^{-1} for rhIDO1, ε_{405} = 159,000 M^{-1} cm^{-1} for the rhIDO1 heme group, and ε_{650} = 195,000 M^{-1} cm^{-1} for the NT650 fluorophore, with a correction factor (F_{corr}) of 0.04 at 280 nm, using C_{prot} = $[A_{280} - (A_{650} \times F_{corr})/\varepsilon_{280l}]$, and DoL resulted between 0.6 and 0.8. Compound predilutions were prepared for MST experiments by 16-fold 1:1 serial dilutions in an assay buffer containing 4% DMSO in PCR tubes supplied by NanoTemper Technologies to yield final volumes of 10 μL. The NT650-rhIDO1 solution was added to each compound dilution and mixed to reach a final NT650-rhIDO1 concentration of 50 nM, including 2% DMSO, 2 mM dithiothreitol (DTT), and a reaction volume of 20 μL. After 10 min of incubation, these samples were loaded into 16 premium-coated capillaries and inserted in the chip tray of the MST instrument for thermophoresis analysis and K_d evaluation. MST signals were recorded at medium MST power and 20% LED power. VS-15 was tested in three independent experiments, and recorded

https://doi.org/10.1021/acsptsci.4c00265
ACS Pharmacol. Transl. Sci. 2024, 7, 3056−3070

data were processed with NanoTemper MO.Affinity Analysis software v2.3 in manual mode setting the hot region between 19 and 20 s. Confidence values (±) are indicated next to the K_d value, showing the range where the K_d value falls with 68% certainty.

Enzymatic Assay. The evaluation of iNOS activity was carried out following the loss of absorbance of NADPH at 340 nm on a Varian Cary 50 Bio UV−Visible Spectrophotometer. The enzymatic assay was performed at 37 °C in a total volume of 150 μL, in the presence of 5 units of recombinant mouse iNOS (Sigma-Aldrich), 65 mM HEPES pH = 7.5, 1.3 mM L-arginine-HCl, 1.3 mM magnesium acetate, 228 μM DTT, and 0.2 mM NADPH. Two minutes after the signal stabilization, iNOS was added to the mix as a reaction starter, and the absorbance at 340 nm was followed for 15 min. To perform the inhibition assay, 5 units of iNOS were preincubated with 10 and 33 μM VS-15 for 3 min at room temperature, and then the complex was added to the reaction mix, as previously described. Every assay was performed in duplicate to provide statistical accuracy. To standardize the enzymatic activity values, the slope of each curve was processed against iNOS standard activity. Then, the iNOS residual activity in the presence of inhibitor VS-15 was calculated.

An IDO1 enzymatic assay was carried out according to the protocol described previously.[46,47] Briefly, compounds dissolved in DMSO (Sigma-Aldrich, MO, USA) or DMSO alone as a control, were added to a standard reaction mixture (130 μL) containing 50 mM potassium phosphate buffer (pH 6.5), 200 μg/mL catalase (Sigma-Aldrich, MO, USA), and 0.125 μg of rhIDO1 protein and allowed to preincubate for the indicated time and temperature (i.e., 15 min at 25 °C or 120 min at 37 °C). After preincubation, 20 μM Trp (Sigma-Aldrich, MO, USA), 20 mM L-ascorbic acid (neutralized with NaOH), and 10 μM methylene blue (Sigma-Aldrich, MO, USA) in 50 mM potassium phosphate buffer (pH 6.5) were added to the reaction (130 μL). The reaction was carried out at 37 °C for 60 min and stopped by the addition of 40 μL of $HClO_4$ (Sigma-Aldrich, MO, USA). To complete the hydrolysis of *N*-formyl-kynurenine into Kyn, samples were heated at 65 °C for 15 min and then centrifuged at 12,000 rpm for 7 min at room temperature. The supernatant (200 μL) was transferred into a new tube and used for Kyn analysis.

***h*IDO1 Heme Displacement Assay.** The enzymatic assay for the displacement of the heme group from recombinant *h*IDO1 was exploited to confirm that VS-15 was an apo-form inhibitor. The cofactor dissociation was followed by measuring the decremental absorbance of the Soret peak at 404 nm for ferric *h*IDO1 on a Varian Cary 50 Bio UV−Visible Spectrophotometer. The assay was performed at 37 °C in a total volume of 200 μL, by testing the inhibitor VS-15 at 10 μM, in the presence of 50 mM phosphate buffer, pH = 7, 1 mM EDTA, 5% DMSO, and 3 μM *h*IDO1. Samples were prepared in 1.5 mL tubes and incubated for 15 min at 37 °C. Then, the heme loss was followed for 30 min.

Succinylacetone Assay. A375 cells were treated with media containing 1 mM tryptophan, 50 μM succinylacetone, and 1000 U/mL of human IFN-γ (PeproTech) to induce IDO1 synthesis and either vehicle (DMSO) or increasing concentrations (0.0001−30 μM) of VS-15 for 48 h. Supernatants were collected, and Kyn levels were measured by HPLC. In each experiment, the corresponding controls were included: IFN-γ treatment alone for the standard assay and IFN-γ plus succinylacetone treatment for the succinylacetone assay.

Evaluation of the Dissociation Constant (K_d) of VS-15 over *h*IDO1. The K_d evaluation assay was optimized to be performed on a 96-well plate (Greiner Bio-One 96-UV-Transparent), following the loss in absorbance at the Soret peak (404 nm) with a Tecan Sunrise 96 Multiplate Reader, at 37 °C for 30 min. The assay was performed by exploiting a serial dilution of the inhibitor VS-15 from 200 to 1.5625 μM, in the presence of 50 mM phosphate buffer, pH = 7, 1 mM EDTA, 5% DMSO, and 3 μM *h*IDO1. Mixtures were assembled in 1.5 mL tubes and incubated for 5 min at 37 °C. Then, the heme absorbance was measured for 30 min. For the calculation of the K_d value, the slope of each curve was plotted against its relative inhibitor concentration, generating a sigmoidal curve, and the final K_d value was calculated by processing raw data in GraphPad, exploiting the Specific Binding with Hill slope tool.

Heme Detection. Free heme in solution was quantified by using a commercially available hemin detection kit (Sigma-Aldrich, MO, USA) as previously described.[25] One μM holo-IDO1 (Giotto Biotech S.r.l., Firenze) in 100 mM potassium phosphate buffer (pH 7.2) plus 1 mM CHAPS was incubated with indicated concentrations of VS-15, epacadostat, or an equivalent volume of DMSO for 120 min at 37 °C. Samples were diluted 100-fold in the provided hemin assay buffer, and the kit reagents were added according to the manufacturer's specifications. Absorbance at 570 nm was measured on a microplate reader (Tecan Trading AG, Switzerland).

Molecular Modeling. All molecular modeling studies were performed on a Tesla workstation equipped with two Intel Xeon X5650 2.67 GHz processors and Ubuntu 20.04 (http://www.ubuntu.com). The protein structures and 3D chemical structures were generated in PyMOL.[48] The structure of compound VS-15 was processed as follows: an in-house script was used to standardize charges, enumerate ionization states, and generate tautomers under the physiological pH range using QUACPAC software from OpenEye.[49] The latter operation was followed by a 3D structure optimization and conformer generation using OMEGA2 software.[26,27] The X-ray structure of the apo-IDO1 complex was used in this study (entry code 6MQ6, chain B).[50] Water molecules were removed, and all hydrogen atoms and MMFF94 charges were added. Then, the complex was transferred into fred_receptor and prepared for docking with FRED.[18] Docked conformations were scored using Chemgauss4.

Immunoprecipitation and Western Blotting. For immunoprecipitation of IDO1, a rabbit monoclonal antimouse IDO1 antibody (CV152) obtained in our laboratory[6] was used. Antibodies used to analyze samples in Western blotting were SH-PTP1 (rabbit polyclonal IgG clone C-19 catalog no. sc-287) and SH-PTP2 (mouse mAb clone B-1 Cat #sc-7384) from Santa Cruz Biotechnology (TX, USA). PI3K p85 (rabbit mAb clone 19H8 Cat. No. 42575) and Rab5 (rabbit mAb clone C8B1 Cat. No. 3547) were from Cell Signaling Technology (MA, USA). β-Tubulin (mouse mAb clone AA2 Cat. No. T8328) was from Sigma-Aldrich (MO, USA).

Cycloheximide-Chase Assay. For the cycloheximide-chase assay, P1.IDO1 cells were pretreated with the protein synthesis inhibitor cycloheximide (Sigma-Aldrich, MO, USA) at the final concentration of 50 μg/mL for 1 h prior to the addition of VS-15 or the vehicle. Cells were then incubated up to 8 h and analyzed by Western blotting.

https://doi.org/10.1021/acsptsci.4c00265
ACS Pharmacol. Transl. Sci. 2024, 7, 3056−3070

Endosome Isolation. Endosomes were isolated using a Minute Endosome Isolation and Cell Fractionation Kit (Invent Biotechnologies, Inc., MN, USA) according to the manufacturer's instructions. Briefly, 3×10^7 cells were collected, washed with cold PBS, and resuspended in buffer A. After incubation, the cell suspension was transferred to a filter cartridge and centrifuged twice. Next, the pellet was resuspended and centrifuged twice. After centrifugation, the supernatant was transferred to a fresh tube, mixed with buffer B, incubated overnight at 4 °C, and centrifuged. The pellet resulting from centrifugation contains isolated endosomes, whereas the supernatant represents the cytosolic fraction. Both fractions were analyzed by Western blotting.

Phosphatase Assay. P1.IDO1 cells were preincubated for 4 h with VS-15 1 μM or DMSO as a control, before assessing the phosphatase activity associated with the IDO1 protein. pDCs were treated overnight with DMSO or TGF-β, in the presence or absence of VS-15 1 μM. For each condition, the IDO1 protein was immunoprecipitated from 6×10^6 cells lysed in 400 μL of lysis buffer (50 mM Tris−HCl pH 7.5, 150 mM NaCl, 1% Nonidet P-40, and a cocktail of protease inhibitors). The IDO1 protein was immunoprecipitated overnight at 4 °C by a specific monoclonal rabbit antibody raised in our lab, followed by the addition of Protein G-Sepharose (Sigma-Aldrich, MO, USA) for 2 h. The phosphatase activity associated with immunoprecipitated IDO1 was assessed by a specific kit purchased from Promega (WI, USA), according to the manufacturer's instructions.

Dendritic Cell Purification and Skin Test Assay. All purification procedures and purities of splenic pDCs and $CD8^-$ DCs (hereafter referred to as cDCs, for conventional DCs) were conducted as previously described.[7,19] Briefly, splenic DCs were purified using CD11c MicroBeads (Miltenyi Biotec) in the presence of EDTA to disrupt DC-T cell complexes. Cells were >99% $CD11c^+$, >99% MHC $I\text{-}A^+$, >98% $B7{-}2^+$, <0.1% $CD3^+$, and appeared to consist of 90−95% $CD8^-$, 5−10% $CD8^+$, and 1−5% $B220^+$ cells. DC populations were further fractionated according to CD8 expression to obtain purified $CD8^+$ and $CD8^-$ DCs using CD8α MicroBeads (Miltenyi Biotec). After cell fractionation, the recovered $CD8^-$ cells typically contained <0.5% contaminating $CD8^+$ DCs, whereas the $CD8^+$ fraction was made up of >95% $CD8^+$ DCs. Less than 3% of $CD11c^+$ cells expressed the mPDCA-1 marker. A skin test assay was used for measurements of major histocompatibility complex class I-restricted delayed-type hypersensitivity (DTH) responses to the HY peptide in C57BL/6 female recipient mice.[51]

For *in vivo* immunization, 3×10^5 peptide-loaded cDCs, combined with a minority fraction (5%) of peptide-loaded pDCs, were injected subcutaneously into recipient mice. After 2 weeks, mice were challenged intrafootpad with the HY peptide in the absence of DCs (experimental footpad) or with the vehicle alone (control counterpart). Twenty-four hours later, mice were sacrificed, footpads were removed, and the change in the weight of the peptide-injected footpad over that of the vehicle-injected counterpart (i.e., internal control) was measured. A significant increase in the mean weight of the experimental footpads over the control footpads will then demonstrate and quantify any delayed-type antigen-specific hypersensitivity response. Representative pictures of the footpads from a positive and negative DTH response have been already published in ref 6. Results are represented as the mean weight ± SD of the experimental footpads over that of control, vehicle-injected counterparts. Measurements were performed in a blinded fashion. The minority cell fraction, constituted by pDCs, was left treated overnight with DMSO or TGF-β, in the presence or absence of VS-15 1 μM.

Real-Time PCR Analysis. Expression of *Ido1* and *Tgfb1* genes was analyzed by real-time PCR, using the specific primers reported previously.[45] Real-time PCR assays were performed using a Stratagene Mx3005P (Agilent Technologies, CA, USA). mRNA levels were normalized to the expression of the *Gapdh* housekeeping gene. The Ct number was measured using MxPro-Mx3005P software (Agilent Technologies, CA, USA). Values were expressed as the ratio of *Gapdh* normalized transcript expression of compound-treated pDCs to *Gapdh* normalized transcript expression.

IDO1 Staining by Flow Cytometry. First, 1×10^6 PBMCs were incubated with FcR Blocking Reagent (Miltenyi Biotec) for 10 min at 4 °C. The following antihuman mAbs were used for surface cell labeling, 30 min at 4 °C: CD14-APC-H7 (MφP9, BD Biosciences), CD16 (3G8, Biolegend), CD3-PerCP-Cy5.5 (UCHT1, BD Biosciences), HLA-DR-PE-Cy7 (L243, Thermo Fisher Scientific), and 0.5 μL LIVE/DEAD Fixable Aqua Stain (Thermo Fisher Scientific). After surface marker staining, PBMCs were fixed and permeabilized with Foxp3/Transcription Factor Staining Buffer Set (eBioscience, Thermo Fisher Scientific), according to the manufacturer's instructions, and incubated with FcR Blocking Reagent for 10 min at room temperature. PBMCs were then incubated for 30 min at 4 °C with a mAb antihuman IDO1-APC (eBioscience, Thermo Fisher Scientific) in permeabilization buffer (eBioscience, Thermo Fisher Scientific). Cells were analyzed by using a BD FACSCanto II system (BD Biosciences) and FlowJo software (Tree Star).

Human Monocyte Viability Assay. Purified monocytes from healthy donors were treated or not treated with increasing concentrations of VS-15. Purified monocytes from tumor patients were treated or not treated with 10 μM VS-15. Following 24 h, cells were stained with Annexin V using Annexin V Apoptosis Detection Kit APC (eBioscience, Thermo Fisher Scientific) and 7-AAD (BD Biosciences). Cell viability was evaluated on $AnnexinV^{neg}7AAD^{neg}$ monocytes by using a BD FACSCanto II system (BD Biosciences) and FlowJo software (Tree Star).

T Cell Proliferation Assay. PBMCs were isolated from leukocytes-enriched buffy coats from healthy donors (Transfusion Centre, University and Hospital Trust of Verona, Italy), stained for 5 min at 37 °C with CellTrace Violet 1 μM (Thermo Fisher Scientific), and protected from light. Labeled PBMCs were stimulated with coated anti-CD3 0.6 μg/mL (clone OKT-3, eBioscience, Thermo Fisher Scientific) and anti-CD28 5 μg/mL (clone CD28.2, eBioscience, Thermo Fisher Scientific) and cocultured for 4 days with tumor-derived circulating monocytes pretreated or not for 24 h with VS-15 10 μM, at a 3:1 ratio (monocytes: PBMCs). Cell cultures were incubated at 37 °C and 8% CO_2 in L-arginine and L-glutamine-free-RPMI (Biochrom), supplemented with L-glutamine 2 mM (Euroclone), L-arginine 150 μM (Sigma-Aldrich), FBS 10% (Superior, Merck), penicillin and streptomycin 10 U/mL (Euroclone), and HEPES 0.1 mM (Euroclone). At the end of the coculture, cells were stained with PE-Cy7 conjugated anti-CD3 (UCHT1, eBioscience, Thermo Fisher Scientific), and CellTrace signals of $CD3^+$ gated lymphocytes were analyzed by flow cytometry and FlowJo software (Tree Star).

https://doi.org/10.1021/acsptsci.4c00265
ACS Pharmacol. Transl. Sci. 2024, 7, 3056−3070

Statistical Analysis. All analyses were performed using Prism version 8.0.1 (GraphPad Software). Data usually met normality and were analyzed by two-tailed paired Student's *t* test when two samples were under comparison or ANOVA followed by posthoc Bonferroni's test when three or more samples were under comparison. A *p*-value of less than 0.05 was considered significant. Overall results, obtained by at least three replicates per experimental parameter, are shown as mean ± SD.

■ ASSOCIATED CONTENT

Data Availability Statement

The data underlying this study are available in the published article and its Supporting Information.

Supporting Information

The Supporting Information is available free of charge at https://pubs.acs.org/doi/10.1021/acsptsci.4c00265.

Additional experimental results, synthesis, characterizations, and ^{1}H NMR and ^{13}C NMR spectra of the compound VS-15 (PDF)

■ AUTHOR INFORMATION

Corresponding Authors

Tracey Pirali − *Department of Pharmaceutical Sciences, University of Piemonte Orientale, Novara 28100, Italy;* orcid.org/0000-0003-3936-4787; Email: tracey.pirali@uniupo.it

Maria Teresa Pallotta − *Pharmacology Section, Department of Medicine and Surgery, University of Perugia, Perugia 06132, Italy;* orcid.org/0000-0002-0417-1638; Email: maria.pallotta@unipg.it

Authors

Eleonora Panfili − *Pharmacology Section, Department of Medicine and Surgery, University of Perugia, Perugia 06132, Italy*

Sarah Jane Rezzi − *Department of Pharmaceutical Sciences, University of Piemonte Orientale, Novara 28100, Italy;* orcid.org/0009-0004-9471-0536

Annalisa Adamo − *Immunology Section, Department of Medicine, University and Hospital Trust of Verona, Verona 37134, Italy*

Daniele Mazzoletti − *Department of Pharmaceutical Sciences, University of Piemonte Orientale, Novara 28100, Italy*

Alberto Massarotti − *Department of Pharmaceutical Sciences, University of Piemonte Orientale, Novara 28100, Italy;* orcid.org/0000-0001-9306-8845

Riccardo Miggiano − *Department of Pharmaceutical Sciences, University of Piemonte Orientale, Novara 28100, Italy*

Silvia Fallarini − *Department of Pharmaceutical Sciences, University of Piemonte Orientale, Novara 28100, Italy*

Sara Ambrosino − *Pharmacology Section, Department of Medicine and Surgery, University of Perugia, Perugia 06132, Italy*

Alice Coletti − *Department of Pharmaceutical Sciences, University of Perugia, Perugia 06132, Italy*

Pasquale Molinaro − *Pharmacology Section, Department of Neuroscience, Reproductive and Dentistry Sciences, School of Medicine, Federico II University of Naples, Naples 80131, Italy*

Michele Milella − *Department of Engineering for Innovative Medicine and Hospital of Trust of Verona, Oncology Section, Verona 37134, Italy*

Salvatore Paiella − *General and Pancreatic Surgery Unit, Pancreas Institute, University of Verona, Verona 37134, Italy*

Antonio Macchiarulo − *Department of Pharmaceutical Sciences, University of Perugia, Perugia 06132, Italy*

Stefano Ugel − *Immunology Section, Department of Medicine, University and Hospital Trust of Verona, Verona 37134, Italy*

Complete contact information is available at: https://pubs.acs.org/10.1021/acsptsci.4c00265

Author Contributions

M.T.P., T.P., S.U., S.F., R.M., P.M.: designed the research; E.P., S.J.R., A.M., S.A., D.M., A.A., A.C.: performed the research; E.P., A.A.: analyzed the data; S.P., M.M.: responsible for biological specimens and patients' data collection; P.M., A.M.: revised the paper; M.T.P., T.P., S.U.: wrote the paper. E.P. and S.J.R. contributed equally to this work.

Notes

The authors declare no competing financial interest.

■ ACKNOWLEDGMENTS

This work was supported by Ministero dell'Università e della Ricerca (PRIN 2022ELLA9L to M.T.P.); Fondazione Italiana per la Ricerca sul Cancro (AIRC): MFAG project: 21509 to S.U. and IG project: 29452 to T.P.; Italian Operational Project (PON) FSE REACT-EU Research and Innovation 2014 2020 Action IV.5 "Dottorati su tematiche green" (DO120P8HZT) to S.J.R.; MUR—M4C2 1.5 of PNRR with grant agreement no. ECS00000036 (project NODES) to T.P.; PNRR programs of the Italian MUR (Project "National Center for Gene Therapy and Drugs Based on RNA Technology", application code CN00000041, Mission 4, Component 2 Investment 1.4, funded from the European Union—NextGeneration EU, MUR Directorial Decree No. 1035 of 17 June 2022, CUP B33C22000630001) to S.U.

■ REFERENCES

(1) Pallotta, M. T.; Rossini, S.; Suvieri, C.; Coletti, A.; Orabona, C.; Macchiarulo, A.; Volpi, C.; Grohmann, U. Indoleamine 2,3-dioxygenase 1 (IDO1): an up-to-date overview of an eclectic immunoregulatory enzyme. *FEBS journal* **2022**, *289* (20), 6099−6118.

(2) Schwarcz, R. The kynurenine pathway of tryptophan degradation as a drug target. *Current opinion in pharmacology* **2004**, *4* (1), 12−17.

(3) Mellor, A. L.; Munn, D. H. IDO expression by dendritic cells: tolerance and tryptophan catabolism. *Nature reviews. Immunology* **2004**, *4* (10), 762−774.

(4) Bessede, A.; Gargaro, M.; Pallotta, M. T.; Matino, D.; Servillo, G.; Brunacci, C.; Bicciato, S.; Mazza, E. M.; Macchiarulo, A.; Vacca, C.; Iannitti, R.; Tissi, L.; Volpi, C.; Belladonna, M. L.; Orabona, C.; Bianchi, R.; Lanz, T. V.; Platten, M.; Della Fazia, M. A.; Piobbico, D.; Puccetti, P. Aryl hydrocarbon receptor control of a disease tolerance defence pathway. *Nature* **2014**, *511* (7508), 184−190.

(5) Gutiérrez-Vázquez, C.; Quintana, F. J. Regulation of the Immune Response by the Aryl Hydrocarbon Receptor. *Immunity* **2018**, *48* (1), 19−33.

(6) Pallotta, M. T.; Orabona, C.; Volpi, C.; Vacca, C.; Belladonna, M. L.; Bianchi, R.; Servillo, G.; Brunacci, C.; Calvitti, M.; Bicciato, S.; Mazza, E. M.; Boon, L.; Grassi, F.; Fioretti, M. C.; Fallarino, F.; Puccetti, P.; Grohmann, U. Indoleamine 2,3-dioxygenase is a signaling

protein in long-term tolerance by dendritic cells. *Nature immunology* **2011**, *12* (9), 870−878.
(7) Mondanelli, G.; Bianchi, R.; Pallotta, M. T.; Orabona, C.; Albini, E.; Iacono, A.; Belladonna, M. L.; Vacca, C.; Fallarino, F.; Macchiarulo, A.; Ugel, S.; Bronte, V.; Gevi, F.; Zolla, L.; Verhaar, A.; Peppelenbosch, M.; Mazza, E. M. C.; Bicciato, S.; Laouar, Y.; Santambrogio, L.; Grohmann, U. A Relay Pathway between Arginine and Tryptophan Metabolism Confers Immunosuppressive Properties on Dendritic Cells. *Immunity* **2017**, *46* (2), 233−244.
(8) Iacono, A.; Pompa, A.; De Marchis, F.; Panfili, E.; Greco, F. A.; Coletti, A.; Orabona, C.; Volpi, C.; Belladonna, M. L.; Mondanelli, G.; Albini, E.; Vacca, C.; Gargaro, M.; Fallarino, F.; Bianchi, R.; De Marcos Lousa, C.; Mazza, E. M.; Bicciato, S.; Proietti, E.; Milano, F.; Pallotta, M. T. Class IA PI3Ks regulate subcellular and functional dynamics of IDO1. *EMBO Rep.* **2020**, *21* (12), No. e49756.
(9) Théate, I.; van Baren, N.; Pilotte, L.; Moulin, P.; Larrieu, P.; Renauld, J. C.; Hervé, C.; Gutierrez-Roelens, I.; Marbaix, E.; Sempoux, C.; Van den Eynde, B. J. Extensive profiling of the expression of the indoleamine 2,3-dioxygenase 1 protein in normal and tumoral human tissues. *Cancer immunology research* **2015**, *3* (2), 161−172.
(10) Brochez, L.; Chevolet, I.; Kruse, V. The rationale of indoleamine 2,3-dioxygenase inhibition for cancer therapy. *European journal of cancer (Oxford, England: 1990)* **2017**, *76*, 167−182.
(11) Peng, X.; Zhao, Z.; Liu, L.; Bai, L.; Tong, R.; Yang, H.; Zhong, L. Targeting Indoleamine Dioxygenase and Tryptophan Dioxygenase in Cancer Immunotherapy: Clinical Progress and Challenges. *Drug design, development and therapy* **2022**, *16*, 2639−2657.
(12) Prendergast, G. C.; Malachowski, W. P.; DuHadaway, J. B.; Muller, A. J. Discovery of IDO1 Inhibitors: From Bench to Bedside. *Cancer research* **2017**, *77* (24), 6795−6811.
(13) Peyraud, F.; Guegan, J. P.; Bodet, D.; Cousin, S.; Bessede, A.; Italiano, A. Targeting Tryptophan Catabolism in Cancer Immunotherapy Era: Challenges and Perspectives. *Frontiers in immunology* **2022**, *13*, No. 807271.
(14) Van den Eynde, B. J.; Baren, N. V.; Baurain, J.-F Is There a Clinical Future for IDO1 Inhibitors After the Failure of Epacadostat in Melanoma? *Annu. Rev. Cancer Biol.* **2020**, *4*, 241−256.
(15) Panfili, E.; Mondanelli, G.; Orabona, C.; Gargaro, M.; Volpi, C.; Belladonna, M. L.; Rossini, S.; Suvieri, C.; Pallotta, M. T. The catalytic inhibitor epacadostat can affect the non-enzymatic function of IDO1. *Frontiers in immunology* **2023**, *14*, No. 1134551.
(16) Serafini, M.; Torre, E.; Aprile, S.; Grosso, E. D.; Gesù, A.; Griglio, A.; Colombo, G.; Travelli, C.; Paiella, S.; Adamo, A.; Orecchini, E.; Coletti, A.; Pallotta, M. T.; Ugel, S.; Massarotti, A.; Pirali, T.; Fallarini, S. Discovery of Highly Potent Benzimidazole Derivatives as Indoleamine 2,3-Dioxygenase-1 (IDO1) Inhibitors: From Structure-Based Virtual Screening to *in Vivo* Pharmacodynamic Activity. *Journal of medicinal chemistry* **2020**, *63* (6), 3047−3065.
(17) Fallarini, S.; Bhela, I. P.; Aprile, S.; Torre, E.; Ranza, A.; Orecchini, E.; Panfili, E.; Pallotta, M. T.; Massarotti, A.; Serafini, M.; Pirali, T. The [1,2,4]Triazolo[4,3-a]pyridine as a New Player in the Field of IDO1 Catalytic Holo-Inhibitors. *ChemMedChem.* **2021**, *16* (22), 3439−3450.
(18) McGann, M. FRED pose prediction and virtual screening accuracy. *J. Chem. Inf. Model.* **2011**, *51* (3), 578−596.
(19) Orabona, C.; Pallotta, M. T.; Volpi, C.; Fallarino, F.; Vacca, C.; Bianchi, R.; Belladonna, M. L.; Fioretti, M. C.; Grohmann, U.; Puccetti, P. SOCS3 drives proteasomal degradation of indoleamine 2,3-dioxygenase (IDO) and antagonizes IDO-dependent tolerogenesis. *Proc. Natl. Acad. Sci. U.S.A.* **2008**, *105* (52), 20828−20833.
(20) Zhong, H. J.; Liu, L. J.; Chong, C. M.; Lu, L.; Wang, M.; Chan, D. S.; Chan, P. W.; Lee, S. M.; Ma, D. L.; Leung, C. H. Discovery of a natural product-like iNOS inhibitor by molecular docking with potential neuroprotective effects in vivo. *PloS one* **2014**, *9* (4), No. e92905.
(21) Adak, S.; Ghosh, S.; Abu-Soud, H. M.; Stuehr, D. J. Role of reductase domain cluster 1 acidic residues in neuronal nitric-oxide synthase. Characterization of the FMN-FREE enzyme. *J. Biol. Chem.* **1999**, *274* (32), 22313−22320.
(22) Nelp, M. T.; Kates, P. A.; Hunt, J. T.; Newitt, J. A.; Balog, A.; Maley, D.; Zhu, X.; Abell, L.; Allentoff, A.; Borzilleri, R.; Lewis, H. A.; Lin, Z.; Seitz, S. P.; Yan, C.; Groves, J. T. Immune-modulating enzyme indoleamine 2,3-dioxygenase is effectively inhibited by targeting its apo-form. *Proc. Natl. Acad. Sci. U.S.A.* **2018**, *115* (13), 3249−3254.
(23) Balog, A.; Lin, T. A.; Maley, D.; Gullo-Brown, J.; Kandoussi, E. H.; Zeng, J.; Hunt, J. T. Preclinical Characterization of Linrodostat Mesylate, a Novel, Potent, and Selective Oral Indoleamine 2,3-Dioxygenase 1 Inhibitor. *Molecular cancer therapeutics* **2021**, *20* (3), 467−476.
(24) Ebert, P. S.; Hess, R. A.; Frykholm, B. C.; Tschudy, D. P. Succinylacetone, a potent inhibitor of heme biosynthesis: effect on cell growth, heme content and delta-aminolevulinic acid dehydratase activity of malignant murine erythroleukemia cells. *Biochemical and biophysical research communications* **1979**, *88* (4), 1382−1390.
(25) Ortiz-Meoz, R. F.; Wang, L.; Matico, R.; Rutkowska-Klute, A.; De la Rosa, M.; Bedard, S.; Midgett, R.; Strohmer, K.; Thomson, D.; Zhang, C.; Mebrahtu, M.; Guss, J.; Totoritis, R.; Consler, T.; Campobasso, N.; Taylor, D.; Lewis, T.; Weaver, K.; Muelbaier, M.; Seal, J.; Zhang, G. Characterization of Apo-Form Selective Inhibition of Indoleamine 2,3-Dioxygenase*. *ChemBioChem* **2021**, *22* (3), 516−522.
(26) Hawkins, P. C.; Nicholls, A. Conformer generation with OMEGA: learning from the data set and the analysis of failures. *J. Chem. Inf. Model.* **2012**, *52* (11), 2919−2936.
(27) Hawkins, P. C.; Skillman, A. G.; Warren, G. L.; Ellingson, B. A.; Stahl, M. T. Conformer generation with OMEGA: algorithm and validation using high quality structures from the Protein Databank and Cambridge Structural Database. *J. Chem. Inf. Model.* **2010**, *50* (4), 572−584.
(28) Röhrig, U. F.; Reynaud, A.; Majjigapu, S. R.; Vogel, P.; Pojer, F.; Zoete, V. Inhibition Mechanisms of Indoleamine 2,3-Dioxygenase 1 (IDO1). *Journal of medicinal chemistry* **2019**, *62* (19), 8784−8795.
(29) Pallotta, M. T.; Orabona, C.; Bianchi, R.; Vacca, C.; Fallarino, F.; Belladonna, M. L.; Volpi, C.; Mondanelli, G.; Gargaro, M.; Allegrucci, M.; Talesa, V. N.; Puccetti, P.; Grohmann, U. Forced IDO1 expression in dendritic cells restores immunoregulatory signalling in autoimmune diabetes. *Journal of cellular and molecular medicine* **2014**, *18* (10), 2082−2091.
(30) Volpi, C.; Fallarino, F.; Pallotta, M. T.; Bianchi, R.; Vacca, C.; Belladonna, M. L.; Orabona, C.; De Luca, A.; Boon, L.; Romani, L.; Grohmann, U.; Puccetti, P. High doses of CpG oligodeoxynucleotides stimulate a tolerogenic TLR9-TRIF pathway. *Nat. Commun.* **2013**, *4*, 1852.
(31) Ugel, S.; Canè, S.; De Sanctis, F.; Bronte, V. Monocytes in the Tumor Microenvironment. *Annual review of pathology* **2021**, *16*, 93−122.
(32) Veglia, F.; Perego, M.; Gabrilovich, D. Myeloid-derived suppressor cells coming of age. *Nature immunology* **2018**, *19* (2), 108−119.
(33) Trovato, R.; Fiore, A.; Sartori, S.; Canè, S.; Giugno, R.; Cascione, L.; Paiella, S.; Salvia, R.; De Sanctis, F.; Poffe, O.; Anselmi, C.; Hofer, F.; Sartoris, S.; Piro, G.; Carbone, C.; Corbo, V.; Lawlor, R.; Solito, S.; Pinton, L.; Mandruzzato, S.; Ugel, S. Immunosuppression by monocytic myeloid-derived suppressor cells in patients with pancreatic ductal carcinoma is orchestrated by STAT3. *J. Immunother. Cancer* **2019**, *7* (1), 255.
(34) Uyttenhove, C.; Pilotte, L.; Théate, I.; Stroobant, V.; Colau, D.; Parmentier, N.; Boon, T.; Van den Eynde, B. J. Evidence for a tumoral immune resistance mechanism based on tryptophan degradation by indoleamine 2,3-dioxygenase. *Nature medicine* **2003**, *9* (10), 1269−1274.
(35) Munn, D. H.; Mellor, A. L. IDO in the Tumor Microenvironment: Inflammation, Counter-Regulation, and Tolerance. *Trends in immunology* **2016**, *37* (3), 193−207.

https://doi.org/10.1021/acsptsci.4c00265
ACS Pharmacol. Transl. Sci. 2024, 7, 3056−3070

(36) Mitchell, T. C.; Hamid, O.; Smith, D. C.; Bauer, T. M.; Wasser, J. S.; Olszanski, A. J.; Luke, J. J.; Balmanoukian, A. S.; Schmidt, E. V.; Zhao, Y.; Gong, X.; Maleski, J.; Leopold, L.; Gajewski, T. F. Epacadostat Plus Pembrolizumab in Patients With Advanced Solid Tumors: Phase I Results From a Multicenter, Open-Label Phase I/II Trial (ECHO-202/KEYNOTE-037). *Journal of clinical oncology: official journal of the American Society of Clinical Oncology* **2018**, *36* (32), 3223−3230.
(37) Zhai, L.; Bell, A.; Ladomersky, E.; Lauing, K. L.; Bollu, L.; Sosman, J. A.; Zhang, B.; Wu, J. D.; Miller, S. D.; Meeks, J. J.; Lukas, R. V.; Wyatt, E.; Doglio, L.; Schiltz, G. E.; McCusker, R. H.; Wainwright, D. A. Immunosuppressive IDO in Cancer: Mechanisms of Action, Animal Models, and Targeting Strategies. *Frontiers in immunology* **2020**, *11*, 1185.
(38) Tang, K.; Wu, Y. H.; Song, Y.; Yu, B. Indoleamine 2,3-dioxygenase 1 (IDO1) inhibitors in clinical trials for cancer immunotherapy. *Journal of hematology & oncology* **2021**, *14* (1), 68.
(39) Zhai, L.; Bell, A.; Ladomersky, E.; Lauing, K. L.; Bollu, L.; Nguyen, B.; Genet, M.; Kim, M.; Chen, P.; Mi, X.; Wu, J. D.; Schipma, M. J.; Wray, B.; Griffiths, J.; Unwin, R. D.; Clark, S. J.; Acharya, R.; Bao, R.; Horbinski, C.; Lukas, R. V.; Wainwright, D. A. Tumor Cell IDO Enhances Immune Suppression and Decreases Survival Independent of Tryptophan Metabolism in Glioblastoma. *Clin. Cancer Res.* **2021**, *27* (23), 6514−6528.
(40) Orecchini, E.; Belladonna, M. L.; Pallotta, M. T.; Volpi, C.; Zizi, L.; Panfili, E.; Gargaro, M.; Fallarino, F.; Rossini, S.; Suvieri, C.; Macchiarulo, A.; Bicciato, S.; Mondanelli, G.; Orabona, C. The signaling function of IDO1 incites the malignant progression of mouse B16 melanoma. *Oncoimmunology* **2023**, *12* (1), No. 2170095.
(41) Rossini, S.; Ambrosino, S.; Volpi, C.; Belladonna, M. L.; Pallotta, M. T.; Panfili, E.; Suvieri, C.; Macchiarulo, A.; Mondanelli, G.; Orabona, C. Epacadostat stabilizes the apo-form of IDO1 and signals a pro-tumorigenic pathway in human ovarian cancer cells. *Front. Immunol.* **2024**, *15*, No. 1346686.
(42) Ladomersky, E.; Zhai, L.; Lauing, K. L.; Bell, A.; Xu, J.; Kocherginsky, M.; Zhang, B.; Wu, J. D.; Podojil, J. R.; Platanias, L. C.; Mochizuki, A. Y.; Prins, R. M.; Kumthekar, P.; Raizer, J. J.; Dixit, K.; Lukas, R. V.; Horbinski, C.; Wei, M.; Zhou, C.; Pawelec, G.; Campisi, J.; Grohmann, U.; Prendergast, G. C.; Munn, D. H.; Wainwright, D. A. Advanced Age Increases Immunosuppression in the Brain and Decreases Immunotherapeutic Efficacy in Subjects with Glioblastoma. *Clin. Cancer Res.* **2020**, *26*, 5232−5245.
(43) Bollu, L. R.; Bommi, P. V.; Monsen, P. J.; Zhai, L.; Lauing, K. L.; Bell, A.; Kim, M.; Ladomersky, E.; Yang, X.; Platanias, L. C.; Matei, D. E.; Bonini, M. G.; Munshi, H. G.; Hashizume, R.; Wu, J. D.; Zhang, B.; James, C. D.; Chen, P.; Kocherginsky, M.; Horbinski, C.; Wainwright, D. A. Identification and Characterization of a Novel Indoleamine 2,3-Dioxygenase 1 Protein Degrader for Glioblastoma. *J. Med. Chem.* **2022**, *65* (23), 15642−15662.
(44) Fallarino, F.; Uyttenhove, C.; Boon, T.; Gajewski, T. F. Endogenous IL-12 is necessary for rejection of P815 tumor variants in vivo. *Journal of immunology (Baltimore, Md.: 1950)* **1996**, *156* (3), 1095−1100.
(45) Albini, E.; Rosini, V.; Gargaro, M.; Mondanelli, G.; Belladonna, M. L.; Pallotta, M. T.; Volpi, C.; Fallarino, F.; Macchiarulo, A.; Antognelli, C.; Bianchi, R.; Vacca, C.; Puccetti, P.; Grohmann, U.; Orabona, C. Distinct roles of immunoreceptor tyrosine-based motifs in immunosuppressive indoleamine 2,3-dioxygenase 1. *Journal of cellular and molecular medicine* **2017**, *21* (1), 165−176.
(46) Albini, E.; Coletti, A.; Greco, F.; Pallotta, M. T.; Mondanelli, G.; Gargaro, M.; Belladonna, M. L.; Volpi, C.; Bianchi, R.; Grohmann, U.; Macchiarulo, A.; Orabona, C. Identification of a 2-propanol analogue modulating the non-enzymatic function of indoleamine 2,3-dioxygenase 1. *Biochemical pharmacology* **2018**, *158*, 286−297.
(47) Austin, C. J.; Mizdrak, J.; Matin, A.; Sirijovski, N.; Kosim-Satyaputra, P.; Willows, R. D.; Roberts, T. H.; Truscott, R. J.; Polekhina, G.; Parker, M. W.; Jamie, J. F. Optimised expression and purification of recombinant human indoleamine 2,3-dioxygenase. *Protein Expression Purif.* **2004**, *37* (2), 392−398.
(48) *The PyMOL Molecular Graphics System, version 2.4.1*; Schrödinger LLC, 2023.
(49) *QUACPAC, version 1.6.3.1*; OpenEye Scientific Software: Santa Fe, NM, http://www.eyesopen.com.
(50) Pham, K. N.; Yeh, S. R. Mapping the Binding Trajectory of a Suicide Inhibitor in Human Indoleamine 2,3-Dioxygenase 1. *J. Am. Chem. Soc.* **2018**, *140* (44), 14538−14541.
(51) Puccetti, P.; Bianchi, R.; Fioretti, M. C.; Ayroldi, E.; Uyttenhove, C.; Van Pel, A.; Boon, T.; Grohmann, U. Use of a skin test assay to determine tumor-specific CD8+ T cell reactivity. *European journal of immunology* **1994**, *24* (6), 1446−1452.

https://doi.org/10.1021/acsptsci.4c00265
ACS Pharmacol. Transl. Sci. 2024, 7, 3056−3070